Journal of Experimental Botany
doi:10.1093/jxb/eraa376 Advance Access Publication 17 August, 2020

RESEARCH PAPER

Ethephon-induced changes in antioxidants and phenolic compounds in anthocyanin-producing black carrot hairy root cultures

Gregorio Barba-Espín[1,2,*], Shih-Ti Chen[1], Sara Agnolet[3], Josefine Nymark Hegelund[1], Jan Stanstrup[3], Jan H. Christensen[3], Renate Müller[1] and Henrik Lütken[1]

[1] Department of Plant and Environmental Sciences, Faculty of Science, University of Copenhagen, 2630 Taastrup, Denmark
[2] Department of Fruit Breeding, CEBAS-CSIC, Campus de Espinardo, 30100 Murcia, Spain
[3] Department of Plant and Environmental Sciences, University of Copenhagen, 1871 Frederiksberg C, Denmark

* Correspondence: gbespin@cebas.csic.es

Received 6 August 2020; Editorial decision 6 August 2020; Accepted 7 August 2020

Editor: Christine Foyer, University of Birmingham, UK

Abstract

Hairy root (HR) cultures are quickly evolving as a fundamental research tool and as a bio-based production system for secondary metabolites. In this study, an efficient protocol for establishment and elicitation of anthocyanin-producing HR cultures from black carrot was established. Taproot and hypocotyl explants of four carrot cultivars were transformed using wild-type *Rhizobium rhizogenes*. HR growth performance on plates was monitored to identify three fast-growing HR lines, two originating from root explants (lines NB-R and 43-R) and one from a hypocotyl explant (line 43-H). The HR biomass accumulated 25- to 30-fold in liquid media over a 4 week period. Nine anthocyanins and 24 hydroxycinnamic acid derivatives were identified and monitored using UPLC-PDA-TOF during HR growth. Adding ethephon, an ethylene-releasing compound, to the HR culture substantially increased the anthocyanin content by up to 82% in line 43-R and hydroxycinnamic acid concentrations by >20% in line NB-R. Moreover, the activities of superoxide dismutase and glutathione *S*-transferase increased in the HRs in response to ethephon, which could be related to the functionality and compartmentalization of anthocyanins. These findings present black carrot HR cultures as a platform for the *in vitro* production of anthocyanins and antioxidants, and provide new insight into the regulation of secondary metabolism in black carrot.

Keywords: Anthocyanins, antioxidant enzymes, black carrot, ethephon, hairy root, hydroxycinnamic acids, *Rhizobium rhizogenes*, *rol* genes.

Introduction

Black carrot (*Daucus carota* L. ssp. *sativus* var. *atrorubens* Alef) accumulates anthocyanins as major secondary metabolites. Due to their high ratio of monoacylated structures with three sugar moieties, black carrot anthocyanins display high chemical stability, which, combined with their elevated concentration in the taproot (Montilla *et al.*, 2011; Barba-Espín *et al.*, 2017), make them suitable replacements for synthetic colourants. Nowadays, extracts of black carrots are commonly used in juices, ice creams, candies, and soft drinks as a healthy alternative to the red azo dye Allura Red (E129) (Carocho *et al.*,

2014). Moreover, as strong dietary antioxidants, anthocyanins help to prevent cardiovascular and neuronal diseases, diabetes, and cancer, among other illnesses (Stintzing and Carle, 2004). In this context, there is substantial potential for new strategies that increase pigment production and thus lower cost-to-value ratio.

Hairy roots (HRs) obtained from the infection of plants by the soil-borne pathogenic bacterium *Rhizobium rhizogenes* (formerly *Agrobacterium rhizogenes*) are evolving fast both as a fundamental research tool and for bio-based production of secondary metabolites in pharmacological, nutraceutical, and cosmetic industries (Bourgaud *et al.*, 2001; Srivastava and Srivastava, 2007; Mishra *et al.*, 2008; Georgiev *et al.*, 2012). HRs have been established from a wide range of plants as a source of secondary metabolites, naturally produced by the plant, or to produce therapeutic recombinant proteins. HRs are also a suitable platform for the study of gene function and to elucidate physiological processes, among other applications (Georgiev *et al.*, 2012; Häkkinen and Oksman-Caldentey, 2018; Gutierrez-Valdes *et al.*, 2020). As a result, the scientific research related to HR cultures has progressively increased since the 1990s, which is also reflected in a number of patents registered in the last few years (Gutierrez-Valdes *et al.*, 2020).

Rhizobium rhizogenes induces the growth of HRs at the infection sites due to the insertion of a plasmid-borne transfer DNA (T-DNA), which, among other genes, contains the four *root oncogenic loci* (*rol*), termed *rolA*, *rolB*, *rolC*, and *rolD* (White *et al.*, 1985; Slightom *et al.*, 1986). When applied as a biotechnological tool, transformation by *R. rhizogenes* results in the development of HRs on the explant material. HRs are characterized by gravitropism loss, profuse growth in the absence of phytohormones, and, often, higher levels of secondary metabolites compared with wild-type roots (Mishra and Ranjan, 2008; Georgiev *et al.*, 2012; Desmet *et al.*, 2020). These distinctive features can be used for marker-free selection of successfully transformed HR lines. Today, there is an increasing awareness that naturally occurring transformation events from *R. rhizogenes* to plants are not confined to a few genera, but are detectable in numerous cultivated and uncultivated plant species (Furner *et al.*, 1986; Matveeva *et al.*, 2012; Kyndt *et al.*, 2015, Matveeva and Otten, 2019).

In agropine strains of *R. rhizogenes*, the T-DNA is split into left (T_L) and right (T_R) fragments. The *rolA–rolD* loci are located on the T_L-DNA, whereas two auxin-homeostasis genes, designated *aux1* and *aux2*, are located on the T_R-DNA (Jouanin *et al.*, 1987). In addition, it has been demonstrated that the two T-DNAs are integrated independently into the host plant genome (Jouanin *et al.*, 1987; Christensen *et al.*, 2008). However, whereas T_L-DNA can be found as single inserts, T_R-DNA has not been detected without the corresponding T_L-DNA in transformed plants or HR lines (Alpizar *et al.*, 2008; Hegelund *et al.*, 2017). Although the mechanism of *rol* gene-mediated induction of HRs is not completely understood, it is hypothesized to involve the activation of signal transduction pathways, including interaction with tyrosine phosphatase and 14-3-3 proteins (Moriuchi *et al.*, 2004). The Western-type carrot (i.e. conventional orange carrot) is highly susceptible to *R. rhizogenes* infection, and routine transformation protocols have been established using taproots as an explant source (Cardarelli *et al.*, 1987; Christey and Braun, 2005). Within a given carrot cultivar, individual biotypes differed in their susceptibility towards the bacterial strain used, which supports the importance of the genotype (Baranski *et al.*, 2006). However, to the best of our knowledge, the *R. rhizogenes*-mediated transformation of black carrot has not been accomplished.

Anthocyanins are regarded as both secondary metabolites and antioxidants (Tanaka *et al.*, 2008). The onset and accumulation of secondary metabolites in HR cultures often requires elicitors (Zhao *et al.*, 2004; Ali *et al.*, 2006; Savitha *et al.*, 2006; Yan *et al.*, 2006; Ahlawat *et al.*, 2014), which usually act as signalling molecules of plant stress responses. The role of ethephon, an ethylene-releasing compound, as an anthocyanin elicitor has been tested in a diverse range of plant organs such as taproots of black carrots (Barba-Espin *et al.*, 2018) and strawberry fruits (Reis *et al.*, 2020), and tartary buckwheat HRs (Li *et al.*, 2017), its effect being linked to a physiological stress response. In this sense, many elicitor treatments have been associated with oxidative stress, which can be a factor directly triggering secondary metabolite formation (Able *et al.*, 2003; Ali *et al.*, 2006; Huerta-Heredia *et al.*, 2009). Upon elicitation, gradual increases in reactive oxygen species (ROS), mainly hydrogen peroxide (H_2O_2), have been reported as stress-mediating signalling molecules (Able *et al.*, 2003). To minimize the harmful effects of ROS, plants have evolved non-enzymatic and enzymatic antioxidant defence mechanisms (Foyer and Noctor, 2011). Anthocyanin accumulation is thus considered a positive response to oxidative stress, since it acts as a non-enzymatic antioxidant capable of directly scavenging ROS (Huda-Faujan *et al.*, 2009). In particular, glutathione *S*-transferases (GST) participate in anthocyanin transportation from the cytoplasm to permanent storage in the vacuole (Edwards *et al.*, 2000). Therefore, elucidating the interplay between the antioxidant system and the secondary metabolism upon elicitation seems to be highly relevant for understanding the accumulation of anthocyanins in HRs.

In the present work, black carrot HRs were induced upon infection with a wild-type *R. rhizogenes* strain. Fast-growing HR lines in combination with the elicitor ethephon were investigated as a platform for the bio-based production of anthocyanins, phenolic compounds, and antioxidants.

Materials and methods

Plant material and explant preparation

Black carrots (*Daucus carota* L. ssp. *sativus* var. *atrorubens* Alef) of two commercial cultivars, 'Deep Purple' F1 and 'Night Bird' F1 (Bejo Seeds Inc., Oceano, CA, USA), and of two inbred lines named 43 and 44 were utilized as explant source. The explants consisted of taproot discs and hypocotyl segments. To obtain taproot discs, 10-week-old taproots grown in a climate chamber under a 12 h photoperiod (20 °C/18 °C) were washed, peeled, and surface sterilized by successive immersion in 70% ethanol, 45 g l^{-1} calcium hypochlorite, and 70% ethanol (for 1, 45, and 1 min, respectively). Finally, the taproots were washed three times in sterile

water and sliced into 0.3–0.5 cm thick discs; the taproot crown (2–4 cm length) was discarded to avoid a high abundance of endophyte species (Surette *et al.*, 2003). To obtain hypocotyl segments, the seeds were *in vitro* germinated on basic medium [BM: 0.22% (w/v) Murashige and Skoog (MS) (Murashige and Skoog, 1962), 3% (w/v) sucrose, 200 mg l^{-1} timentin (ticarcillin disodium:potassium clavulanate, 15:1; Duchefa Biochemie, Haarlem, The Netherlands), and 400 µl l^{-1} Atamon containing $NaC_6H_5CO_2$ (Haugen-group, Hvidovre, Denmark)]. Twelve-day-old hypocotyls were excised into 5 cm length segments, producing fresh wounds for inoculation.

Induction and maintenance of hairy roots

Rhizobium rhizogenes strain A4, harbouring the agropine-type plasmid pRiA4, was cultured into 50 ml of MYA [0.4% mannitol, 0.5% (w/v) yeast extract, 0.05% (w/v) casamino acids, and 0.2% (w/v) ammonium sulfate, pH 6.6] in the dark at 180 rpm and 28 °C (Hegelund *et al.*, 2017). At an OD_{600}=0.65, the bacterial suspension was in the logarithmic phase and ready for inoculation.

Surface-sterilized explants were immersed in the bacterial culture solution for 30 min. As control, explants were immersed in MYA without bacteria. Following inoculation, explants were washed in sterile water and blotted with sterilized filter paper to remove excess bacteria. After 2 d of co-cultivation on solid 0.22% (w/v) half-strength MS (1/2 MS) containing 15 mg l^{-1} acetosyringone (Sigma–Aldrich Co., St. Louis, MO, USA), the explants were transferred onto solid BM (four explants per plate). Two to four weeks after inoculation, HRs that formed at the wound sites of the root discs and hypocotyl segments were transferred individually onto solid BM and subsequently propagated via subcultures on 1/2 MS medium every 3 weeks. In addition, a few non-inoculated explants developed adventitious roots (data not shown), characterized by low branching and vigour, which made them easily separable from putatively transformed HRs. As a source of inoculum for all experiments, HR segments were grown in the dark in 250 ml flasks containing 100 ml of 1/2 MS for 1 week at 100 rpm on an oscillatory shaker (Innova 4430, New Brunswick Scientific, Enfield, CT, USA).

Based on their distinctive morphology, >90 viable HR lines were first designated as putatively transformed. Out of these lines, the three showing the most vigorous growth on solid medium after 5–7 subcultures, namely NB-R, 43-R, and 43-H, originating from a root explant of carrot 'Night Bird' F1, a root explant of carrot 43, and a hypocotyl explant of carrot 43, respectively, were selected for molecular confirmation of transformation and further experiments.

Extraction of DNA and RNA, and PCR analysis

Genomic DNA and RNA from 100 mg of tissue were extracted with a DNeasy Plant Mini Kit and RNeasy Plant Minikit (Qiagen, Venlo, The Netherlands), respectively, according to the manufacturer's instructions. DNA and RNA yield and purity were determined by a Nanodro™ 1000 spectrophotometer (Thermo Fisher Scientific Inc., Waltham, MA, USA). RNA integrity was verified on agarose gels. Purified RNA was stored at −80 °C. Subsequently, 1 µg of RNA was treated with Amplification Grade DNase I (Sigma–Aldrich Co.) and cDNA synthesized using an iScript cDNA synthesis kit (Bio-Rad, Hercules, CA, USA), as recommended by the supplier. All PCRs using gDNA or cDNA were performed using Ex Taq polymerase (Takara Bio Inc., Kusatsu, Japan), as recommended by the manufacturer, with addition of 2% (v/v) DMSO in the final reactions. Primers targeting *rolB*, *aux1*, and *aux2* were used as indicators of the presence of T_L- and T_R-DNA, respectively (Lütken *et al.*, 2012). Primers targeting *VirD2* were used to detect any residual bacteria remaining on the hairy roots. Primers targeting carrot *DcActin1* was used as a control (Wang *et al.*, 2016; Barba-Espín *et al.*, 2017). With the exception of *rolA-D*, where annealing temperatures were 1 min at 55.6 °C, the PCR conditions were as follows: 4 min at 94 °C, 35 cycles of [30 s 94 °C, 1 min 60 °C, 45 s 72 °C], and 72 °C at 7 min. Primer pairs were evaluated for PCR and quantitative real-time PCR (RT-qPCR) analyses. The primer nucleotide sequences are specified in Supplementary Table S1 at JXB online).

Quantitative real-time PCR analyses

RT-qPCR was performed using SsoAdvanced™ Universal SYBR® Green Supermix according to the manufacturer's instructions (Bio-Rad) with a CFX Connect™ Real-Time PCR Detection System (Bio-Rad). Analyses of primer temperature optimization, melting curves, standard curves for primer pair efficiencies, Cq values, and normalized expression (ΔΔCq) in addition to reference primer pair selection were conducted using CFX Maestro Software (Bio-Rad). Specific RT-qPCR settings and efficiencies for primers targeting *rolA–rolD* (Lütken *et al.*, 2012) and reference genes (Wang *et al.*, 2016) are available in Supplementary Table S2. The experimental design included three technical replicates and three biological replicates. Negative and non-reverse transcription controls were included where relevant. The RT-qPCR assay was duplicated in full from the level of HR cultures.

Cultivation in liquid cultures and ethephon application

The culture conditions consisted of 12 h light (140 µmol m^{-2} s^{-1})/12 h darkness (20 °C/18 °C) on an oscillatory shaker at 100 rpm (Innova 4430, New Brunswick Scientific). The HR inoculum (0.3–0.35 g FW of a 1 week pre-culture) was transferred to 250 ml glass Erlenmeyer flasks containing 100 ml of liquid MS at different strengths (1/4 MS, 1/2 MS, and full MS), where a time-course analysis of biomass accumulation and anthocyanin content was conducted over a 4 week period. Subsequently, based on the highest yield obtained in 1/2 MS, this medium was chosen for investigating the effect of ethephon (Sigma–Aldrich Co.). A 100 mg ml^{-1} ethephon (Sigma–Aldrich Co.) stock solution was prepared and added to HR cultures in 1/2 MS medium at day 0 or 10, resulting in final concentrations of 50 mg l^{-1} and 200 mg l^{-1} for both days of application.

The whole HR from each flask (biological replicate) was collected at different time points (0, 5, 10, 15, 21, and 28 d), then washed, blotted, weighed, frozen in liquid nitrogen, and stored at −80 °C until further analysis. The experimental design included at least five biological replicates.

Determination of total monomeric anthocyanin content (TMAC)

HRs were homogenized in a 3% sulfuric acid solution (1:1, w/w), using a Waring® two-speed commercial blender (VWR, Bie & Berntsen, Herlev, Denmark). Subsequently, the generated homogenate was thoroughly mixed with distilled water (1:2, w/w). After 1 h incubation at room temperature, the mix was centrifuged for 20 min at 4000 *g*. The supernatant (extract) was used to determine the TMAC according to the pH differential method with slight modifications (Barba-Espín *et al.*, 2017). In brief, the HR extract was diluted in 0.2 M KCl–HCl pH 1 (1:20, v/v), and the absorption of the mix was registered between 700 nm and 350 nm using a UV-visible spectrophotometer (Thermo Scientific Evolution™ 220, Waltham, MA, USA). TMAC was calculated as cyanidin-3-glucoside equivalents.

Extraction procedure and sample preparation for ultra-high performance liquid chromatography-photodiode array detector mass spectrometry (UPLC-PDA-TOF MS)

HRs were freeze-dried for 24 h using a ScanVac Freeze Dryer CoolSafe 4 Touch (LaboGene, Alleroed, Denmark). Subsequently, the dried material was ground into powder using a mortar. Upon an initial extraction screening on a composite HR sample (data not shown), the following high extraction efficiency protocol was established: 50 mg of the HR powder was extracted twice in 1.5 ml of a 50% methanol (HPLC grade, Chemsolute®, Roskilde, Denmark) solution with 1% formic acid (Chemsolute®), and once in 1 ml of the same solution. The extract was then vortexed, sonicated, and centrifuged for 10 min at 10 000 *g* (Hettich® MIKRO 120 centrifuge, Thermo Fisher Scientific, MA, USA). The supernatant generated in the successive extractions (4 ml) was filtered through Hydrophilic 0.20 µm membrane filters (Millex Samplicity Filter, Merck, Darmstadt, Germany) and used for analysis. Extractions were carried out on five biological replicates. A quality control (QC)

sample consisting of a pool of equivalent aliquots of the individual extracts was prepared.

Identification and quantification of phenolic compounds by UHPLC-PDA-TOF MS

Polyphenols were identified and quantified by means of UHPLC-PDA-TOF MS. Chromatography was performed on an Acquity UPLC I-Class system (Waters Corp., Milford, MA, USA) equipped with a Binary Solvent Manager (BSM), a Sample Manager with a Flow Through Needle (SM-FTN), and a Column Manager. The system was then coupled to a Waters 2998 photodiode array detector (PDA) and a Xevo G2 TOF mass spectrometer with an electrospray ionization (ESI) source (Waters Corp.). Separation was obtained on an Acquity UPLC BEH C18 column (130 Å, 1.7 µm, 2.1 mm×100 mm) (Waters Corp.) maintained at 40 °C. The mobile phase consisted of 1% formic acid in water, v/v (eluent A), and 1% formic acid in methanol (LC-MS grade, MikroLab Aarhus A/S, Hoejbjerg, Denmark), v/v (eluent B). The gradient elution program was as follows: 0 min, 1% B; 15 min, 30% B; 25 min, 99% B; 27 min, 99% B; 27.1 min, 1% B; and 30 min, 1% B. The flow rate was 0.4 ml min^{-1}, and the injection volume was 6 µl. QCs were used to monitor technical variation. All extracts and QC samples were diluted twice with water before injection, performed in random order. UV/Vis absorption spectra were recorded from 210 nm to 600 nm in steps of 1.2 nm at a sampling rate of 5 points s^{-1}. Hydroxycinnamic derivatives (detected at 330 nm) and anthocyanins (detected at 520 nm) were quantified as chlorogenic acid and cyanidin-3-*O*-glucoside equivalents g DW^{-1}, respectively, using external standard calibration curves (Extrasynthese, Lyon, France).

The full-scan mass spectra were recorded in positive ESI mode for all samples and in both positive and negative ionization mode for QCs and selected samples, for which MS^E data were also obtained. The source parameters were as follows: capillary voltage, 2.0 kV; cone voltage, 30 V; source temperature, 120 °C; desolvation temperature, 500 °C; cone gas flow rate, 50 l h^{-1}; and desolvation gas flow rate, 900 l h^{-1}. The scan range was from 100 *m/z* to 1000 *m/z* with 0.5 s scan time, a 0.014 s inter-scan delay, and 6 eV collision energy. For MS^E experiments, function 1, at low energy, was registered with a collision energy of 10 eV, and function 2, at high energy, was acquired with a collision energy ramp from 10 eV to 50 eV. Data were recorded in centroid mode. All analyses were performed using 50 pg μl^{-1} leucine-enkephalin (Sigma–Aldrich Co.) as lockmass introduced by a lockspray at 20 µl min^{-1} and measured every 30 s. Compound identification was based on comparison with authentic standards. If standards were unavailable, a tentative identification was reported based on previous literature, retention time consideration, and mass spectral data. All operations were controlled by MassLynx version 4.1 software (Waters Corp., Milford, MA, USA).

UHPLC-PDA-TOF MS data pre-processing and method validation

LC-UV/VIS-MS data were converted to mzML using msconvert from ProteoWizard and imported into R using the R package mzR (Kessner *et al.*, 2008; Chambers *et al.*, 2012). The UV/VIS traces for 520 nm and 330 nm (±2 nm) were extracted and baseline corrected using the rollingBall algorithm in the baseline package (Liland *et al.*, 2010). The CentWave algorithm in XCMS (Smith *et al.*, 2006; Tautenhahn *et al.*, 2008) was used to detect all untargeted peaks; subsequently, 33 pre-specified peaks (specified by retention time and wavelength) were selected. The integration for each peak was then manually inspected graphically.

The LC-UV/VIS analytical method developed for the quantitative analysis of anthocyanins and hydroxycinnamic acid derivatives was validated in terms of linearity, limit of detection (LOD), limit of quantitation (LOQ), precision (intraday and interday repeatability tests), and accuracy. The linearity of calibration curves for chlorogenic acid and cyanidin-3-*O*-glucoside was evaluated by the coefficient of determination (R^2) and the residuals of the fitted regression models. A weighted linear regression within the working concentration range (0.2–370 mg l^{-1}) was used (R^2>0.99). The low end of the concentration range (0.2–5 mg l^{-1}) employed a standard linear regression model and was used to establish LOD and LOQ. The intraday and interday precision were evaluated by repeated injections of samples and standards performed on the same days and on different days, respectively, during data acquisition. QC samples, used to monitor technical variation, were analysed along the entire sequence. The coefficient of variation for all experiments did not exceed 10%. Accuracy was determined by the addition of standards at two concentrations into three different samples, which resulted in average recoveries of 92–102%.

Determination of antioxidant enzyme activity

Enzyme extractions were performed according to Acosta-Motos *et al.* (2017). In brief, HR samples were homogenized (1:2, w/v) in 50 mM Tris–acetate buffer containing 0.1 mM EDTA, 2 mM cysteine, and 0.2% (v/v) Triton X-100 (pH 6.0). The extracts were centrifuged for 15 min at 10 000 *g* (Hettich Mikro 120, Fisher Scientific, Pittsburgh, PA, USA). Finally, the supernatant was filtered on Sephadex G-25 NAP columns according to the manufacturer's instructions (GE Healthcare, Chicago, IL, USA). The protein concentration was determined according to Bradford (1976), and the activities of catalase (CAT), peroxidase (POD), superoxide dismutase (SOD), and GST were assayed as described by Clemente-Moreno *et al.* (2009) and Barba-Espin *et al.* (2012). The analyses were conducted using a UV/Vis V-630 Bio spectrophotometer (Jasco, Tokyo, Japan).

Statistical analysis

All analyses were done with at least five biological replicates (independent HRs), except for RT-qPCR, in which case three biological replicates were included. All experiments were conducted independently twice. Data were expressed as the mean ±SE. Statistical analyses for qPCR were done in CFX Maestro (Bio-Rad) using one-way ANOVA followed by Tukey's post-hoc test ($P \leq 0.05$). For the rest of the analyses, the Statistical Package for the Social Sciences (SPSS Statistics 19.0, IBM Corp., Armonk, NY, USA) was used, and one-way ANOVA was performed followed either by Tukey's post-hoc test or by Student's *t*-test for pairwise comparisons ($P \leq 0.05$).

Results and discussion

Establishment and selection of black carrot hairy root lines

An efficient transformation procedure in black carrots was established by screening *R. rhizogenes*-mediated transformation efficiencies in four cultivars and two explant types—taproot discs and hypocotyl segments (Fig. 1). Ninety-two HRs were isolated and classified as putatively transformed due to their characteristic phenotype (Tepfer, 1984). Transformation efficiencies were higher for taproot than for hypocotyl explants, ranging from 26% (for cv. 44) to 85% (for 'Night Bird' F1). In contrast, the frequencies of the HRs from hypocotyls were notably lower, displaying values between 3.7% (for 'Deep Purple' F1) and 12% (for cv. 43). This is in contrast to earlier findings in which young tissues, such as hypocotyls, young leaves, and cotyledons, provided high transformation frequencies (Sevón and Oksman-Caldentey, 2002). On the other hand, transformation frequency was in the range of that observed by Baranski *et al.* (2006) upon a broad comparison of 12 Western carrot genotypes and four *R. rhizogenes* strains. Figure 2 shows the development of the HRs on explants and the subsequent transfer to axenic culture. Interestingly, a number of the HR cultures displayed the presence of bacterial and fungal contaminants

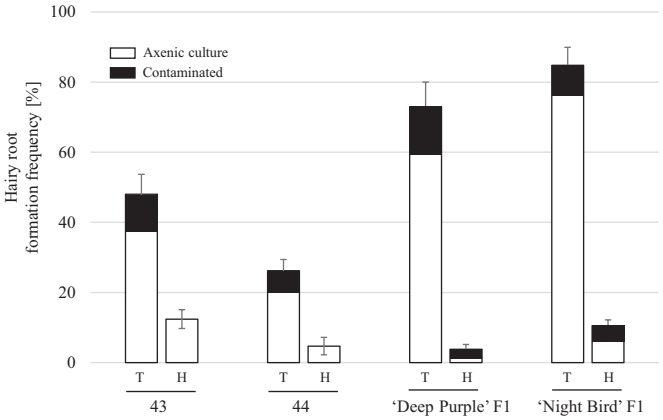

Fig. 1. Hairy root formation frequency (%) on taproot (T) and hypocotyl (H) explants from four black carrot cultivars (43, 44, 'Deep Purple' F1, and 'Night Bird' F1). Percentages represent the number of hairy root clusters per hundred explants. Error bars represent the SE of two independent transformation experiments.

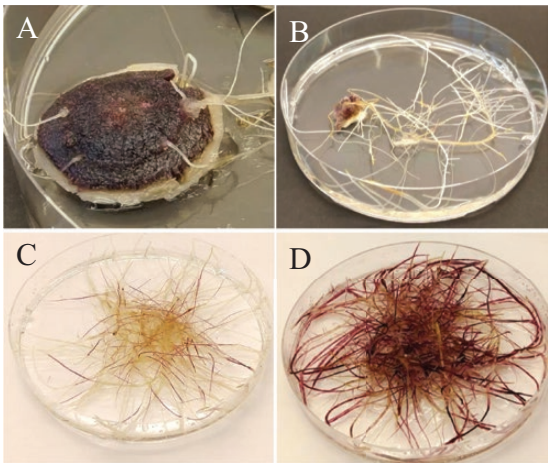

Fig. 2. Representative pictures of hairy root emergence and growth performance on 1/2 MS solid medium. Line NB-R, originated from a carrot disc explant 3 weeks after *Rhizobium rhizogenes* inoculation (A), was excised and transferred onto BM (B). After 3 weeks of culture on 1/2 MS medium, hairy roots incubated in darkness displayed weaker pigmentation (C) compared with hairy roots incubated under a 12 h photoperiod (D). (This figure is available in colour at *JXB* online.)

(Fig. 1). In a parallel study, these contaminants were identified as culturable endophyte species (unpublished results), which supports recent findings regarding endophyte abundance in carrot (Nan *et al.*, 2019; Abdelrazek *et al.*, 2020).

Among the HR lines generated, lines NB-R, 43-R, and 43-H—originating from a root explant of 'Night Bird', a root explant of 43, and a hypocotyl explant of 43, respectively—were selected on the basis of their prolific growth and branching growth habit in Petri dishes. These HR lines were confirmed to be transformed by PCR (Fig. 3) and then selected for further experiments in glass Erlenmeyer flasks. Integration of T_L-DNA in the three lines was verified by the detection of *rolB* and the absence of *virD2*, which is located on the pRiA4 plasmid but not in the transferred region. Interestingly, none of the selected HR lines contained *aux* genes, which belong to T_R-DNA (Fig. 3). This was previously observed in carrot

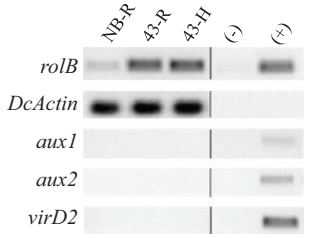

Fig. 3. PCR fragments of *rolB*, *aux1*, *aux2*, *DcActin*, and *VirD2* in the carrot hairy root lines NB-R, 43-R, and 43-H. (–), negative control (water); (+), positive control (pRiA4).

transformed with different *R. rhizogenes* strains, where a majority of the HR lines generated did not contain T_R-DNA (Capone *et al.*, 1989). Similarly, root cultures of coffee showed no integration of T_R-DNA among 55 tested root lines (Alpizar *et al.*, 2008).

Influence of medium strength on hairy root growth and anthocyanin content

The impact of MS medium strengths, namely 1/4, 1/2, and full MS, was evaluated on the growth and TMAC of the three HR lines cultivated for a 12 h photoperiod over a 4 week period (Fig. 4). Incubation in darkness was not included as it provided similar biomass accumulation but low or absent pigmentation (Fig. 2C). Similarly, Abbasi *et al.* (2007) reported a light-enhanced accumulation of anthocyanin in HR cultures of *Echinacea purpurea*. In our study, a growth kinetic resembling a sigmoidal curve was displayed in the three HR lines grown in different media, where an initial lag phase was followed by a log phase and, finally, a plateau phase at day 21 (Fig. 4A–C). The biomass achieved was higher in 1/2 and full MS (Fig. 4B, C) than in 1/4 MS (Fig. 4A). Nevertheless, medium strength did not show a drastic effect on HR growth, which supports earlier observations that HRs are less susceptible to changes in medium strength than cell suspension and callus cultures (Sáenz-Carbonell *et al.*, 1997; Giri *et al.*, 2001). At day 28, line 43-H in 1/2 MS reached the highest yield, displaying increases of 28.9% and 39.3% with respect to the corresponding yields of 43-R and NB-R. The 25- to 30-fold increases in biomass in the course of 28 d were higher than those published in HRs from orange carrot (Kondo *et al.*, 1989; Baranski *et al.*, 2006; Sircar *et al.*, 2007), and they are in the range of the highest yields obtained in flasks (e.g. *Rubia akane*; Park and Lee, 2009) and in bioreactors (e.g. *Panax ginseng*; Yu *et al.*, 2005).

In contrast to its minor effect on biomass, medium strength strongly influenced anthocyanin production (Fig. 4D-F). Overall, HRs grown in 1/4 and 1/2 MS displayed a typical S-shaped anthocyanin production curve, although TMAC was moderately higher in 1/2 MS, in which case the levels were 4- to 6-fold higher than those in full MS. This discrepancy may be due to excess nutrition in the latter medium (Yin *et al.*, 2013). Comparable results were also reported by Yu *et al.* (2000), who found that lower medium strengths favoured ginsenoside accumulation, whereas maximum biomass was obtained in full MS. Maximum TMAC (3.03 ± 0.10 mg g^{-1} DW) was achieved in line 43-R at day 28

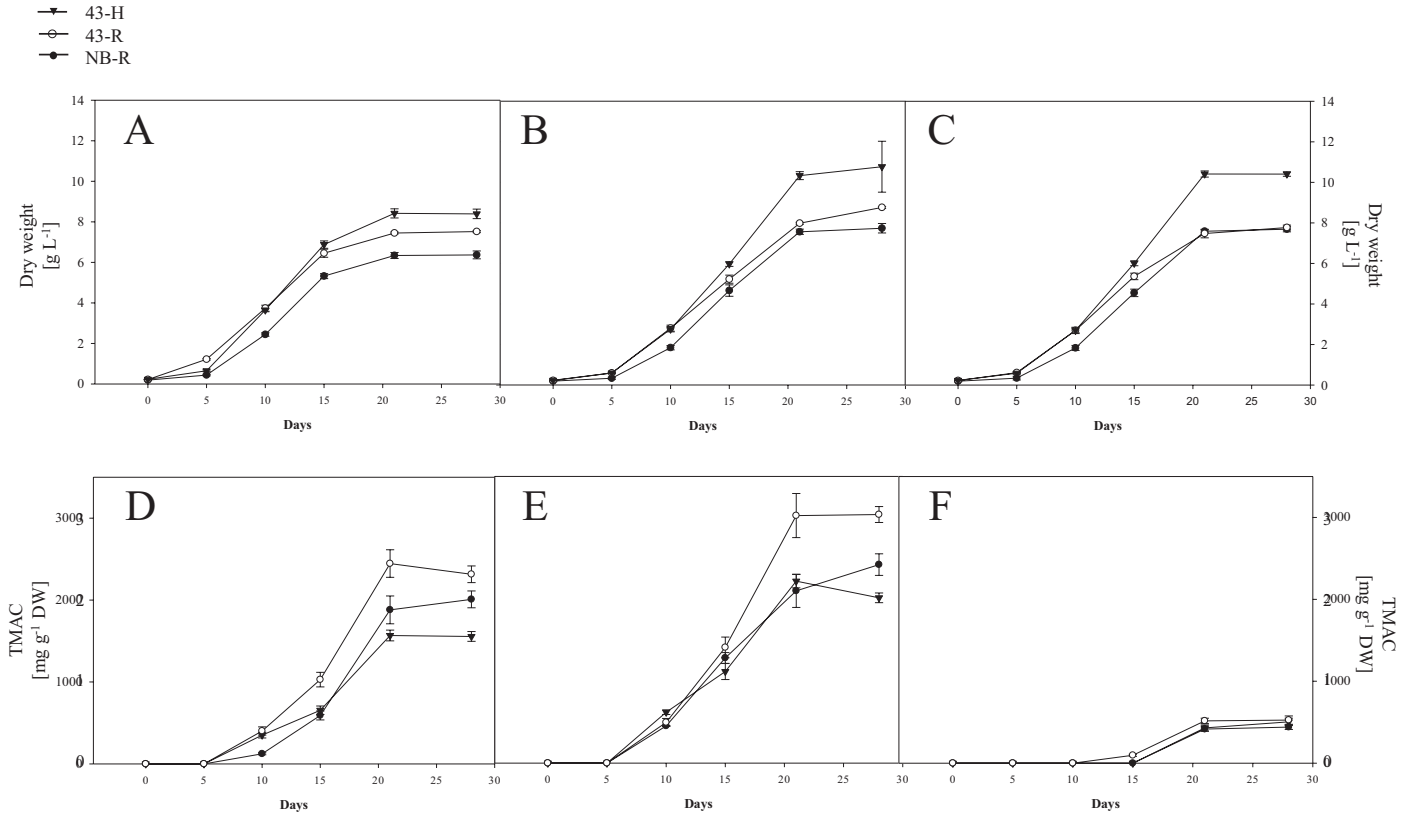

Fig. 4. Biomass accumulation (g DW l^{-1}) and total monomeric anthocyanin content (TMAC) of the selected hairy root lines in 1/4 MS (A, D), 1/2 MS (B, E), and full MS (C, F) liquid media over a 4 week period. Data represent the mean ±SE, *n*=5.

(Fig. 4E). Overall, the similar S-shaped curves of biomass and anthocyanin production indicate that there was not a clear separation in time between biomass formation and the functioning of secondary metabolism, as reported in two-step *in vitro* production systems (Guerriero *et al.*, 2018). Altogether, the cultivation of HR in 1/2 MS was found to be suitable for both biomass and anthocyanin accumulation.

Ethephon as an anthocyanin elicitor in hairy roots

The effect of the ethylene-releasing chemical, ethephon, as an anthocyanin elicitor was previously reported in taproots of black carrot (Barba-Espín *et al.*, 2017), where an increased expression of anthocyanin biosynthesis genes in response to ethephon treatment was observed. Similarly, ethephon increased the betalain contents of beetroot, with no detrimental effect on root size (Barba-Espin *et al.*, 2018). Anthocyanin accumulation was also enhanced 3-fold in tartary buckwheat HRs treated with ethephon (Li *et al.*, 2017). In the present work, the capacity of ethephon as an anthocyanin elicitor was tested in 1/2 MS medium. First, two ethephon concentrations (50 mg l^{-1} and 200 mg l^{-1}) and two application times (day 0 or 10) were tested in line 43-H, and their effect was analysed at the end of the 28 d period (Fig. 5). The lower concentration did not change biomass or anthocyanin content when added either at day 0 or day 10. In contrast, 200 mg l^{-1} ethephon triggered a distinct response as a function of the application time: when applied at day 0, ethephon decreased both DW and TMAC by 40% and 20%, respectively, whereas application

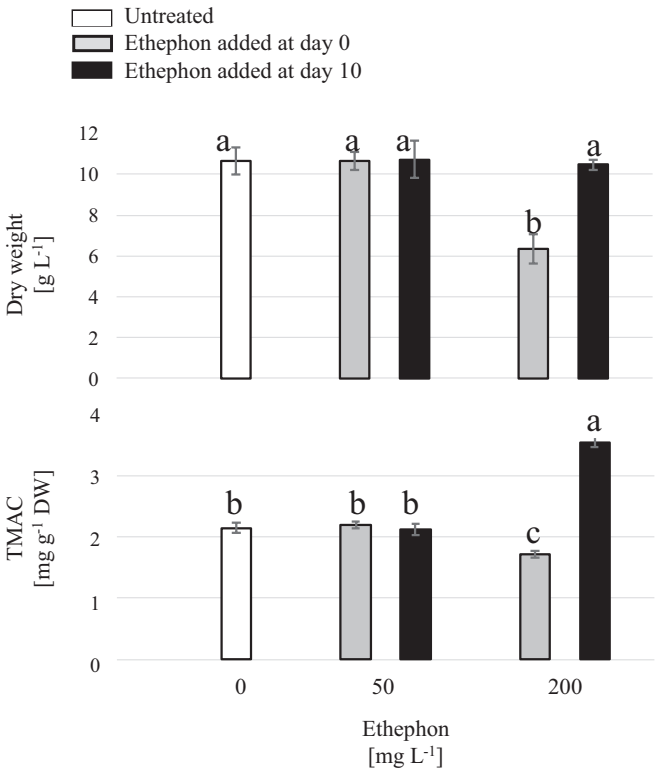

Fig. 5. Effect of ethephon concentration (50 mg l^{-1} or 200 mg l^{-1}) and time of application (day 0 or 10) on the g DW l^{-1} and total monomeric anthocyanin content (TMAC) of hairy roots of 43-H measured at day 28. Different letters indicate statistical significance according to Tukey's test ($P \leq 0.05$). Data represent the mean ±SE, *n*=5.

at day 10 increased TMAC by 65% with no detrimental effect on the biomass (Fig. 5). The importance of the age of the culture in elicitation was previously shown in HR culture of *Whitania somnifera* (Sivanandhan *et al.*, 2013) and in cell cultures of *Catharanthus roseus* (Namdeo *et al.*, 2004; Gautam *et al.*, 2011), where earlier applications of elicitor negatively affected bioactive compound accumulation. This phenomenon can be explained by a less efficient enzymatic machinery and, thereby, a reduced elicitor response in early phases of growth (Kombrink *et al.*, 1986; Vasconsuelo *et al.*, 2003).

Monitoring anthocyanin and phenolic composition in ethephon-treated hairy root

Based on the results in the above-mentioned analyses, 200 mg l^{-1} ethephon applied at day 10 was chosen for further experiments, and its effect was monitored during the growth of lines 43-R, 43-H, and NB-R. Ethephon-treated HRs displayed a more intensive and uniform pigmentation (Fig. 6A), particularly on the abaxial surface. Such differential colouration may relate to the different light prevalence throughout the

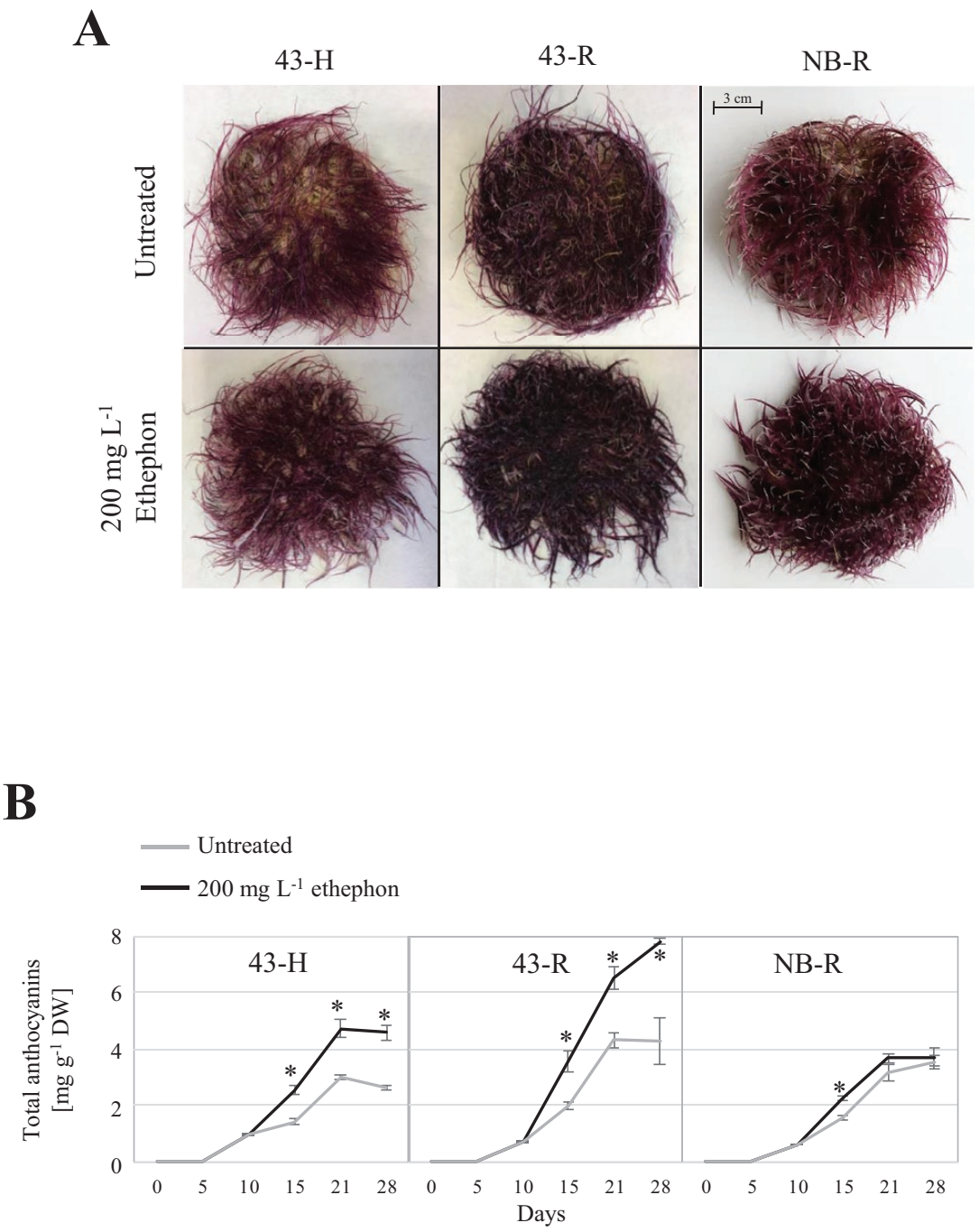

Fig. 6. Effect of ethephon on anthocyanin accumulation in 43-H, 43-R, and NB-R hairy root lines. (A) Image of untreated and 200 mg l^{-1} ethephon-treated hairy roots at day 28. (B) Total anthocyanins based on quantification of individual anthocyanin forms by UPLC-PDA. Data represent the mean ±SE, n=5. Asterisks indicate significant differences between untreated and treated samples for each pairwise comparison according to Student's t-test ($P \leq 0.05$). (This figure is available in colour at *JXB* online.)

HR, given that light is one of the main factors stimulating anthocyanin biosynthesis (Toguri *et al.*, 1993; Chalker-Scott, 1999). No significant changes in biomass were found between ethephon-treated and untreated HRs at any sampling point (data not shown).

Anthocyanins and other phenolic compounds were identified by UHPLC-PDA-TOF MS in samples of the three HR lines in response to the ethephon treatment. In total, nine anthocyanin compounds were characterized based on accurate mass and fragmentation patterns, retention time, and comparison with previous literature (Table 1; Figs 7, 8). Two non-acylated (peaks A1 and A2) and five acylated (peaks A3-A7) cyanidin-based forms were found, as reported in black carrot taproot (Kammerer *et al.*, 2003; Montilla *et al.*, 2011; Algarra *et al.*, 2014). The characteristic fragment at m/z 287, corresponding to cyanidin aglycone, confirmed the assignment. Two other anthocyanins, present in trace amounts, were tentatively assigned (peak A8) as peonidin 3-xyloxyl(sinapoylglucosyl) galactoside (m/z 963) and peonidin 3-xyloxyl(feruloylglucosyl) galactoside (m/z 933), for which the characteristic peonidin aglycone fragment at m/z 301 was detected. Based on the abundance of each individual anthocyanin form, the total anthocyanin content was calculated over the 4 week period (Fig. 6B). Compared with untreated HRs, the mean anthocyanin content was higher in the elicited HRs of the three lines at days 15, 20, and 28. In 43-R, the total anthocyanin content reached an 82% increase upon elicitation at day 28. The corresponding increase in 43-H at day 28 was 75%. In NB-R, however, the most pronounced difference between treated and untreated HRs was found at day 15 (45%), and this difference decreased to 16% by day 28. Compared with anthocyanin determination by TMAC measurement (Figs 4E, 5), MS quantification provided higher concentrations, and the differences between methods ranged from 25% to 30% (data not shown). Such differences can be attributed to a higher extraction efficiency of samples for UHPLC-PDA-TOF MS.

The percentage of acylated forms (peaks A3–A8) increased over time in both treated and untreated HRs, as occurs during black carrot taproot development (Barba-Espín *et al.*, 2017). At day 28, acylated forms ranged from 78% (untreated 43-H) to 84% (treated NB-R) (data not shown), which contrasts with the 50–60% prevalence in mature black carrot taproots (Montilla *et al.*, 2011; Algarra *et al.*, 2014; Barba-Espín *et al.*, 2017). This highlights the potential applicability of black carrot HRs in colourant production, as acylated anthocyanins show increased stability in downstream applications (Giusti and Wrolstad, 2003; Fenger *et al.*, 2019).

The most prevalent anthocyanin in black carrot taproot corresponds to cyanidin 3-xylosyl(feruloylglucosyl)galactoside (Kammerer *et al.*, 2003), which was the major acylated anthocyanin detected in lines 43-H and NB-R. Conversely, cyanidin 3-xylosyl(sinapoylglucosyl)galactoside (peak A5) was the most abundant form in 43-R, and the level increased by >133% in elicitor-treated HRs compared with untreated HRs (Fig. 7). This indicates differential regulation in response to ethephon among HR lines, even though 43-H and 43-R originated from the same carrot cultivar. However, the mechanisms that determine changes in the anthocyanin composition pattern in black carrot have not yet been clarified.

Regarding non-anthocyanin phenolic compounds, 24-hydroxycinnamic acid derivatives were identified based on accurate mass and fragmentation patterns, retention time, and comparison with previous literature in black carrot (Alasalvar *et al.*, 2001; Kammerer *et al.*, 2004; Ceoldo *et al.*, 2009) (Table 2; Supplementary Tables S3, S4; Figs 9, 10). Individual phenolic compounds differ considerably in their contribution to total antioxidant capacity (Goupy *et al.*, 2003; Sroka *et al.*, 2003). Most importantly, hydroxycinnamic acid derivatives contribute to anthocyanin stability in black carrot by intermolecular co-pigmentation (Cortez *et al.*, 2016). Based on the content of individual hydroxycinnamic compounds, the total hydroxycinnamic acid content was calculated (Fig. 9). The levels reached were in the range of the highest phenolic contents reported to date in black carrot (Algarra *et al.*, 2014; Barba-Espín *et al.*, 2017), and an order of magnitude greater than the anthocyanin contents reported in this study (Fig. 6B). Ethephon elicitation increased the hydroxycinnamic compound content solely in NB-R, reaching 64.2±2.28 mg g^{-1} DW and 52.6±1.93 mg g^{-1} DW in treated and untreated HRs, respectively (Fig. 9).

Among hydroxycinnamic acids, chlorogenic acid was the major compound in NB-R (peak P2), as reported in black

Table 1. Identification of anthocyanins in the hairy root extracts of lines 43-H, 43-R, and NB-R by LC-MS in positive ESI mode

Peak no.	Rt (min)	Tentative identification	Exact mass (m/z) $[M]^+$	Measured mass (m/z) $[M]^+$	Δm (ppm)	Major fragments
A1	8.30	Cyanidin 3-xylosyl(glucosyl)galactoside	743.2035	743.2024	1.5	287.0567
A2	8.80	Cyanidin 3-xylosylgalactoside	581.1506	581.1507	0.2	287.0636
A3	9.13	Cyanidin 3-xylosyl(caffeoylglucosyl)galactoside	905.2352	905.2346	0.7	287.0567
A4	10.06	Cyanidin 3-xylosyl(hydroxybenzoylglucosyl) galactoside	863.2246	863.2272	3.0	287.0567
A5	10.36	Cyanidin 3-xylosyl(sinapoylglucosyl)galactoside	949.2614	949.2614	0.0	287.0550
A6	10.80	Cyanidin 3-xylosyl(feruloylglucosyl)galactoside	919.2508	919.2504	0.4	287.0550
A7	11.10	Cyanidin 3-xylosyl(coumaroylglucosyl)galactoside	889.2402	889.2368	3.8	287.0580
A8	11.45	Peonidin 3-xylosil (sinapoylglucosyl) galactoside	963.2765	963.2791	2.7	301.0726
		Peonidin 3-xylosil (feruloylglcucosyl) galactoside	933.2659	933.2627	3.4	301.0726

Peaks correspond to those indicated in Fig. 8.

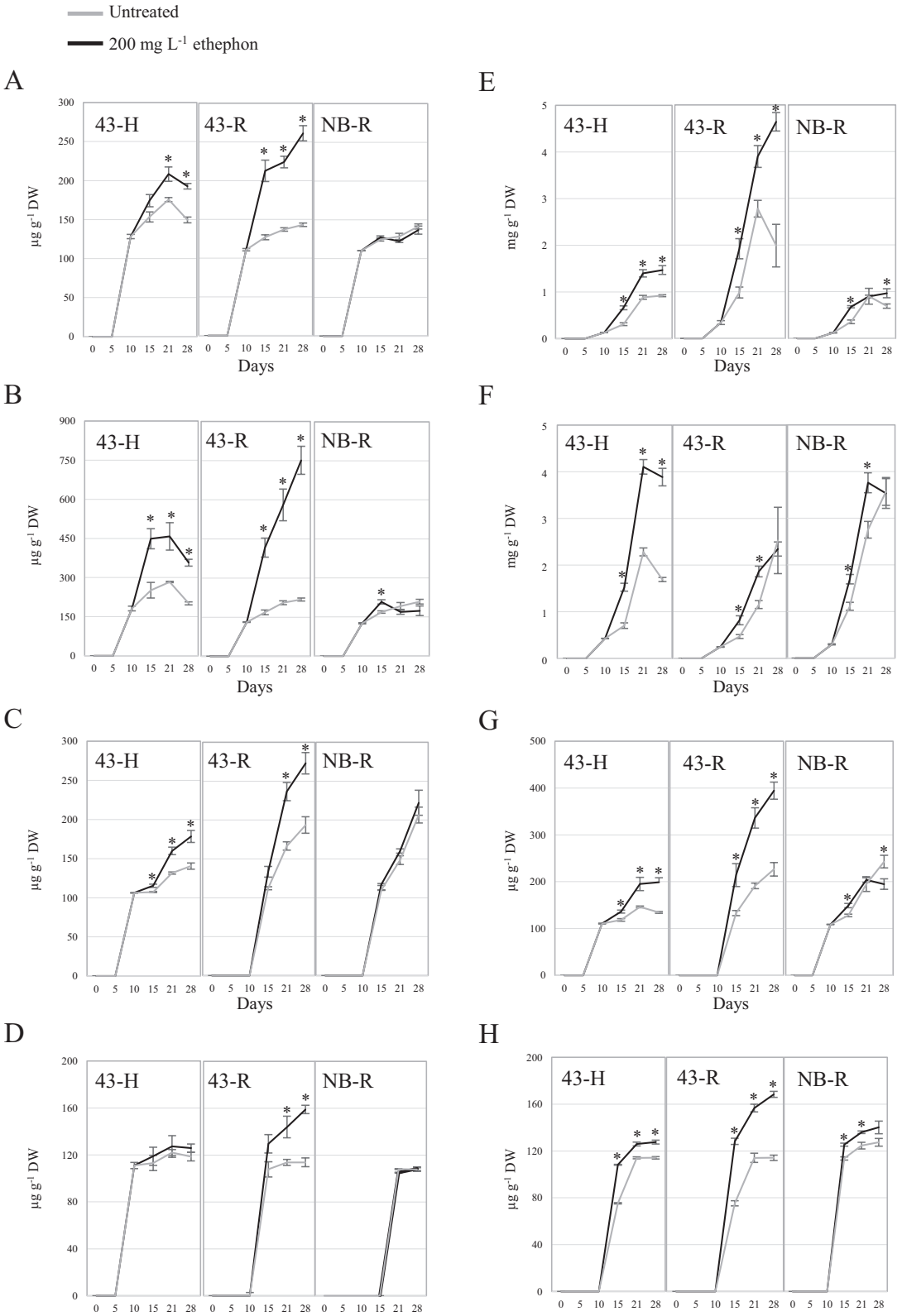

Fig. 7. Anthocyanin composition monitored in untreated and 200 mg l^{-1} ethephon-treated hairy roots of 43-H, 43-R, and NB-R. Anthocyanin forms are displayed according to elution order (A–H): (A) cyanidin 3-xylosyl(glucosyl)galactoside; (B) cyanidin 3-xylosylgalactoside; (C) cyanidin 3-xylosyl(caffeoylglucosyl)galactoside; (D) cyanidin 3-xylosyl(hydroxybenzoylglucosyl)galactoside; (E) cyanidin 3-xylosyl(sinapoylglucosyl)galactoside; (F) cyanidin 3-xylosyl(feruloylglucosyl)galactoside; (G) cyanidin 3-xylosyl(coumaroylglucosyl)galactoside; and (H) peonidin-3-xylosyl(feruloylglucosyl) galactoside and peonidin 3-xylosil (sinapoylglucosyl) galactoside. Data represent the mean ±SE, *n*=5. Asterisks indicate significant differences between untreated and treated samples for each pairwise comparison according to Student's *t*-test ($P \leq 0.05$).

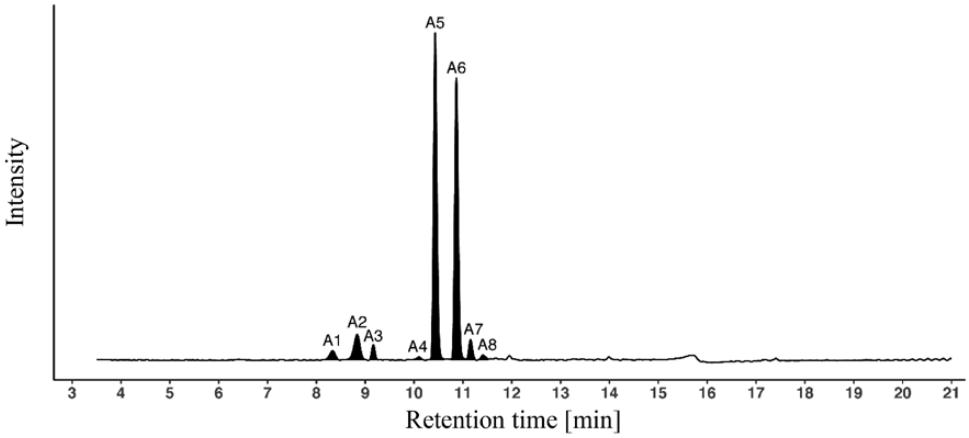

Fig. 8. Typical LC-UV/VIS trace of anthocyanins in black carrot hairy roots recorded at 520 nm. Peak identification (A1–A8) is shown in Table 1.

Table 2. Identification of hydroxycinnamic acid derivatives in the hairy root extracts of lines 43-H, 43-R, and NB-R by LC-MS in negative ESI mode

Peak no.	Rt (min)	Tentative identification	Exact mass (*m/z*) $[M-H]^-$	Measured mass (*m/z*) $[M-H]^-$	Δm (ppm)	Major fragments
P1	4.38	Caffeoyldaucic acid	365.0514	365.0522	2.2	203.0173 $[M\text{-caffeoyl-H}]^-$, 731.1066 $[2M-H]^-$
P2	6.39	Chlorogenic acid[a]	353.0878	353.0870	2.3	191.0530 $[M\text{-caffeoyl-H}]^-$, 707.1830 $[2M-H]^-$
P3	7.17	Caffeoylhexoside	341.0878	341.0858	5.9	179.0354 $[M\text{-hexose-H}]^-$
P4	7.75	Feruloylhexoside	355.1034	355.1029	1.4	193.0511 $[M\text{-hexose-H}]^-$, 175.0394 $[M\text{-hexose-H}_2O]^-$
P5	8.51	Sinapoylhexoside	385.1140	385.1130	2.6	223.0605 $[M\text{-hexose-H}]^-$, 205.0490 $[M\text{-hexose-H}_2O]^-$
P6	8.81	Caffeoylquinic acid	353.0878	353.0829	13.9	191.0519 $[M\text{-caffeoyl-H}]^-$
P7	9.97	Feruloylquinic acid	367.1034	367.1016	4.9	191.0528 $[M\text{-feruloyl-H}]^-$, 735.2131 $[2M-H]^-$
P8	11.88	Caffeoyldaucic acid	365.0514	365.0507	1.9	203.0180 $[M\text{-caffeoyl-H}]^-$, 185.0087 $[M\text{-caffeoyl-water-H}]^-$, 731.1066 $[2M-H]^-$
P9	12.10	Feruloylquinic acid	367.1034	367.1027	1.9	191.0548 $[M\text{-feruloyl-H}]^-$
P10	14.06	Unknown	–	–	–	–
P11	14.37	Dicaffeoylquinic acid	515.1195	515.1191	0.8	353.0880 $[M\text{-caffeoyl-H}]^-$
P12	14.78	Feruloyldaucic acid derivative	–	–	–	379.0658 [feruloyldaucic acid-H]$^-$
P13	15.50	Dicaffeoyldaucic acid	527.0831	527.0807	4.6	365.0494 $[M\text{-caffeoyl-H}]^-$, 203.0170 $[M\text{-(2*caffeoyl)-H}]^-$, 185.0086 $[M\text{-(2*caffeoyl)-water-H}]^-$
P14	16.40	Dicaffeoylquinic acid	515.1195	515.1158	7.2	353.0838 $[M\text{-caffeoyl-H}]^-$
P15	16.97	Caffeoylferuloyldaucic acid	541.0987	541.0975	2.2	379.0650 $[M\text{-caffeoyl-H}]^-$, 365.0500 $[M\text{-feruloyl-H}]^-$, 203.0199 $[M\text{-caffeoyl-feruloyl-H}]^-$, 185.0107 $[M\text{-caffeoyl-feruloyl-water-H}]^-$, 179.0346 [caffeic acid-H]$^-$
P16	17.23	Caffeoylsinapoyldaucic acid	571.1093	571.1118	4.4	409.0792 $[M\text{-caffeoyl-H}]^-$, 203.0191 $[M\text{-caffeoyl-sinapoyl-H}]^-$, 185.0091 $[M\text{-caffeoyl-sinapoyl-water-H}]^-$
		Dicaffeoyldaucic acid	527.0831	527.0834	0.6	365.0509 $[M\text{-caffeoyl-H}]^-$, 203.0191 $[M\text{-(2*caffeoyl)-H}]^-$, 185.0091 $[M\text{-(2*caffeoyl)-water-H}]^-$
P17	17.40	Caffeoylferuloyldaucic acid	541.0987	541.0988	0.2	379.0675 $[M\text{-caffeoyl-H}]^-$, 203.0204 $[M\text{-caffeoyl-feruloyl-H}]^-$, 185.0093 $[M\text{-caffeoyl-feruloyl-water-H}]^-$
		Caffeoylsinapoylquinic acid	559.1457	559.1461	0.7	397.1143 $[M\text{-caffeoyl-H}]^-$
P18	17.61	Caffeoylferuloylquinic acid	529.1351	529.1326	4.7	353.0846 $[M\text{-feruloyl-H}]^-$
P19	17.78	Dicaffeoylquinic acid	515.1195	515.1187	1.6	353.0872 $[M\text{-caffeoyl-H}]^-$
P20	17.99	Diferuloyldaucic acid	555.1144	555.1136	1.4	379.0675 $[M\text{-feruloyl-H}]^-$, 193.0504 [M-feruloyldaucic acid-H]$^-$
P21	18.17	Feruloylsinapoylquinic acid	573.1613	573.1604	1.6	397.1151 $[M\text{-feruloyl-H}]^-$
P22	18.29	Diferuloyl quinic acid	543.1508	543.1492	2.9	367.0995 $[M\text{-feruloyl-H}]^-$
P23	18.50	Caffeoylferuloyl quinic acid	529.1351	529.1346	0.9	367.1011 $[M\text{-caffeoyl-H}]^-$, 353.0854 $[M\text{-feruloyl-H}]^-$
P24	18.73	Unknown	–	–	–	–
P25	20.34	Unknown	–	–	–	–

Peaks correspond to those indicated in Fig. 10.

HRMS data along with neutral loos information were used for the identification of hydroxicinnamic acid derivatives (common neutral losses used for the identification of the sugar moiety and acyl groups were: caffeoyl, *m/z* 162.0317; hexose, *m/z* 162.0528; feruloyl, *m/z* 176.0473; sinapoyl, *m/z* 206.0579).

[a] Peak was identified by matching the retention time and *m/z* value with the authentic standard.

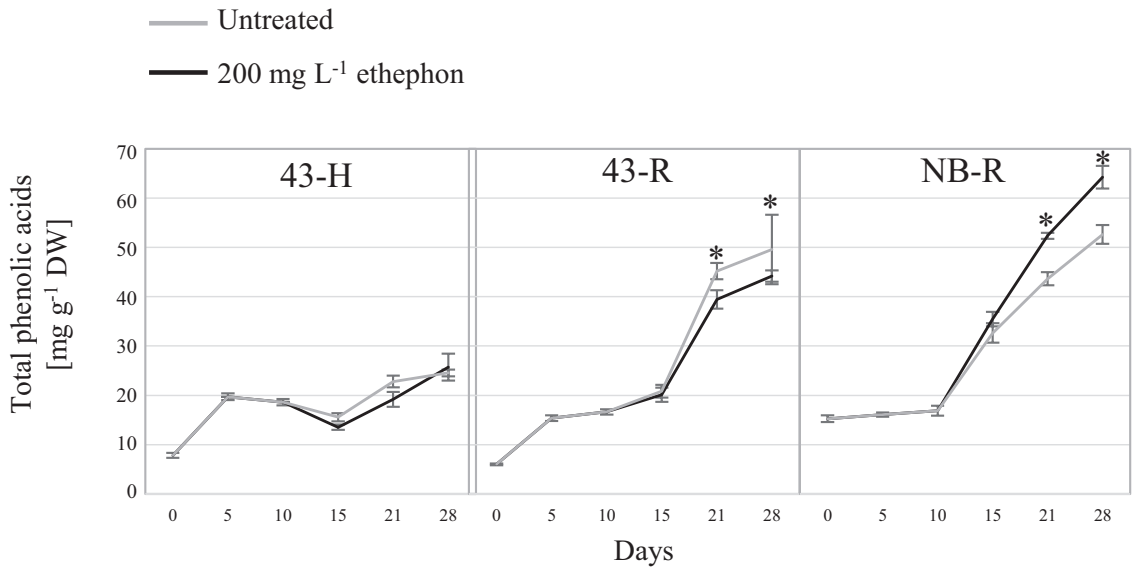

Fig. 9. Accumulation of hydroxycinnamic acid derivatives in untreated and 200 mg l^{-1} ethephon-treated hairy roots of 43-H, 43-R, and NB-R over a 4 week period. Data represent the mean ±SE, *n*=5. Asterisks indicate significant differences between untreated and treated samples for each pairwise comparison according to Student's *t*-test ($P \leq 0.05$).

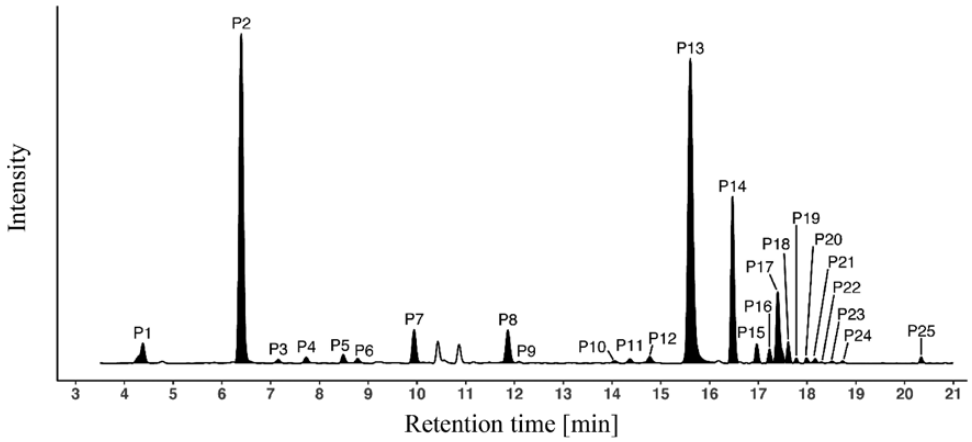

Fig. 10. Typical LC-UV/VIS trace of non-anthocyanin phenolic compounds in black carrot hairy roots recorded at 330 nm. Peak identification (P1–P25) is shown in Table 2.

carrot taproot (Alasalvar *et al.*, 2001; Kammerer *et al.*, 2004), whereas the predominant phenolic acid in 43-H and 43-R consisted of dicaffeoyldaucic acid (peak P13) (Table 2; Supplementary Table S4). Among the most abundant compounds observed, namely chlorogenic acid (peak P2), dicaffeoyldaucic acid (peak P13), dicaffeoylquinic acid (peak P14), caffeoylferuloyldaucic acid and caffeoylsinapoylquinic acid (joint elution in peak P17), and caffeoylferuloylquinic acid (peak P18), NB-R displayed remarkable increases upon elicitation for peaks P13, P14, P17, and P18 (35, 31, 62, and 81%, respectively) (Table 2; Supplementary Table S4). For 43-H, only chlorogenic acid increased in treated HRs, from 4.88±0.14 mg g^{-1} DW to 6.30±0.83 mg g^{-1} DW. In comparison, the same compound in 43-R decreased by 31% upon elicitation. Taken together, it seems that, in addition to the effect of carrot genotype (Baranski *et al.*, 2006), individual transformation events within the same genotype may lead to distinct patterns of secondary metabolites.

Antioxidant enzyme activities over time and in response to ethephon

The activity of the main antioxidant enzymes was studied in the HRs in order to correlate changes in these enzymes with changes in growth and anthocyanin accumulation (Fig. 11). The plant antioxidant system is composed of enzymatic and non-enzymatic components and is responsible for maintaining a tight balance between ROS production and scavenging (Mittler *et al.*, 2002). Among the enzymatic components, SOD generates H_2O_2 from superoxide radicals ($O_2^{\cdot -}$), whereas CAT and peroxidases catalyse the scavenging of H_2O_2 (Mittler *et al.*, 2002; Díaz-Vivancos *et al.*, 2010). In addition to their role as detoxifiers of diverse exogenous substrates, multiple GST enzymes display glutathione peroxidase activity, thus these GSTs participate in antioxidative metabolism by reducing lipid hydroperoxides and scavenging H_2O_2 (Bartling *et al.*, 1993; Dixon *et al.*, 2009). Importantly, certain GSTs are

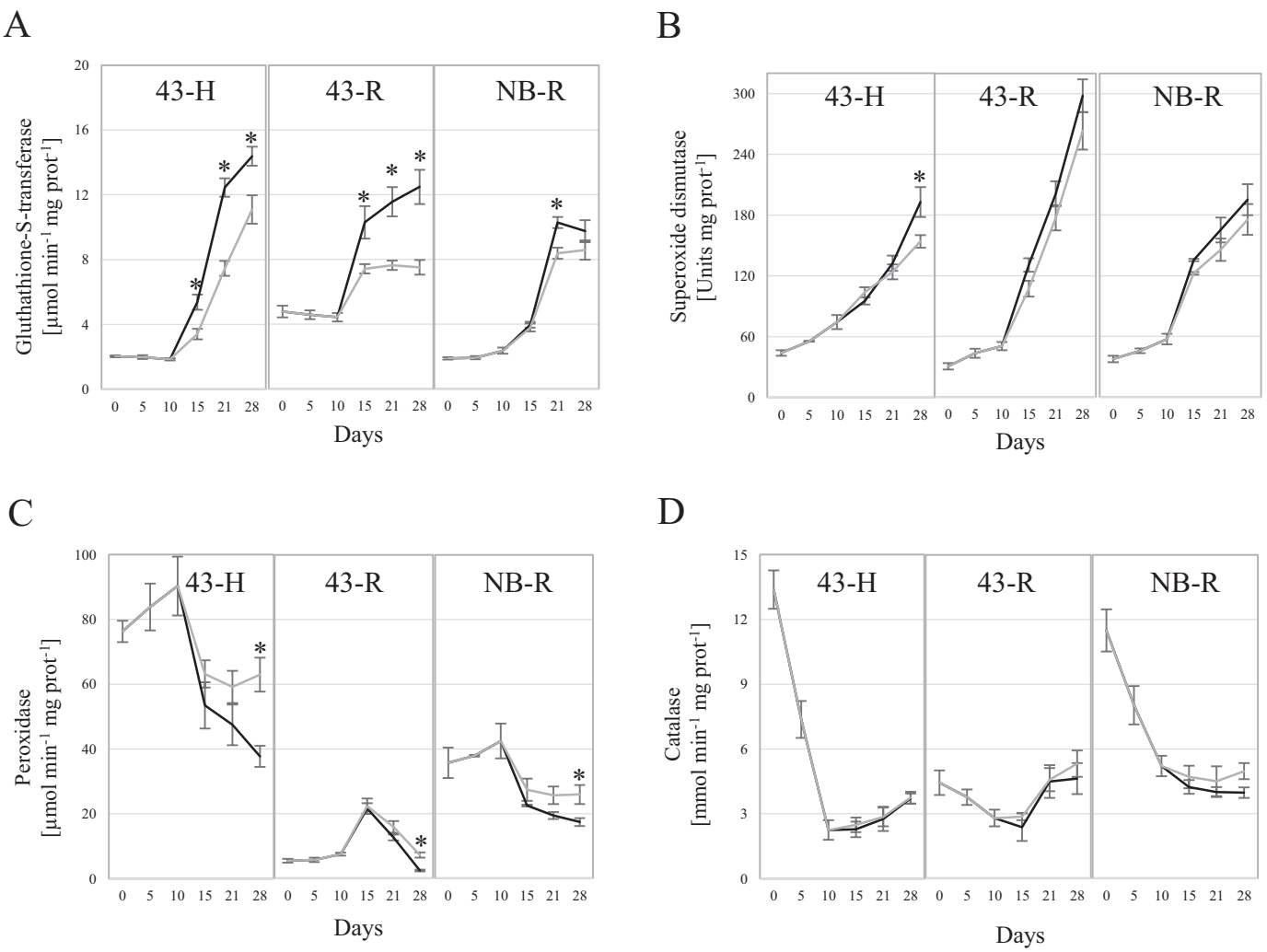

Fig. 11. Antioxidant enzyme activities monitored in untreated and 200 mg l^{-1} ethephon-treated hairy roots of 43-H, 43-R, and NB-R. Data represent the mean ±SE, *n*=5. Asterisks indicate significant differences between untreated and treated samples for each pairwise comparison according to Student's *t*-test ($P \leq 0.05$).

necessary for efficient anthocyanin transport from the cytoplasm into permanent sequestration in the vacuole (Edwards *et al.*, 2000; Behrens *et al.*, 2019). The increased GST activity observed over time and in response to ethephon elicitation in the three HR lines (Fig. 11A) may therefore correlate to anthocyanin accumulation in the vacuole. In 43-H, the GST activity increased from 2.03±0.06 µmol min^{-1} mg $protein^{-1}$ at day 0 to 14.38±0.59 and 11.09±0.88 µmol min^{-1} mg $protein^{-1}$ at day 28 in ethephon-treated and untreated HRs, respectively. Nevertheless, it seems that GSTs involved in transportation do not catalyse anthocyanin glutathionation, but rather bind reversibly to anthocyanins, acting as carrier proteins (Zhao *et al.*, 2015; Behrens *et al.*, 2019). The increase in SOD activity over time (Fig. 11B) would result in H_2O_2 production. In this sense, expression of *rol* genes has been associated with an oxidative burst leading to increased secondary metabolite production in *Rubia cordifolia* (Bulgakov *et al.*, 2008). Moreover, biotic and abiotic elicitation has been found to stimulate the antioxidant system via an oxidative burst in HRs of different species (Goel *et al.*, 2011). In the present study, such a defence response against a hypothetical ROS burst was not reflected in a stimulation of POD (Fig. 11C or CAT (Fig. 11D) activities. Instead, anthocyanins, as powerful non-enzymatic antioxidants capable of directly scavenging ROS (Huda-Faujan *et al.*, 2009), could be modulating the excess H_2O_2 generated by SOD activity. In addition, increased GST activity in elicited HRs could be related to the glutathione peroxidase activity of certain GSTs (Dixon *et al.*, 2009). Although ROS are mainly produced in the cytoplasm, mitochondria, and peroxisome, they can diffuse across cell membranes, especially H_2O_2, and enter into vacuoles (Yamasaki *et al.*, 1997; Mubarakshina *et al.*, 2010). In vacuoles, there is no SOD or CAT, and ROS scavenging relies mainly on non-enzymatic antioxidants (Mittler *et al.*, 2004). Moreover, although mostly described as cytosolic proteins, GSTs have been

found to be associated with the vacuole among other organelles (Carter *et al.*, 2004; Heazlewood *et al.*, 2004; Zybailov *et al.*, 2008). Consequently, anthocyanin and GSTs located in the vacuole could be critical in maintaining homeostasis in the HRs over time and in response to ethephon.

Expression analysis of rolA–rolD *in hairy roots*

To investigate whether ethephon treatment influenced the expression levels of *rol* genes, 15-day-old HRs of 43-H and 43-R were analysed by RT-qPCR. This growth stage was used as it was the first sampling point after ethephon application. Transcripts of all four T-DNA-localized *rol* genes could be confirmed; however, none of the *rolA-D* transcript levels was found to respond to the ethephon treatment (Fig. 12). Among the transferred genes, *rolA*, *B*, and *C* or their combination have been found to induce HRs in numerous species, including carrot (Shkryl *et al.*, 2007), and synergistic effects of the *rol* genes on an enhanced production of secondary metabolites have been reported (Giri and Narasu, 2000; Sevón and Oksman-Caldentey, 2002; Shkryl *et al.*, 2007). However, it remains unknown whether secondary metabolite production is linked to differential expression levels of *rol* genes. In the present study, differential patterns of secondary metabolism in response to ethephon were observed in two lines, 43-H and 43-R, which both originated from the same carrot cultivar. However, this did not correlate with any ethephon-induced changes in the transcription of *rol* genes (Fig. 12).

Genetic stability of HRs is well known (Georgiev *et al.*, 2012; Desmet *et al.*, 2020). In the present study, the expression analysis was done >2 years after obtaining the HR lines, in parallel with the determination of the antioxidant enzyme activities and the anthocyanin and phenolic composition. During that time, >30 regular subculturings were done. Moreover, the three selected HR lines were maintained for nearly 4 years via regular subculturing without measured loss of vigour and pigmentation. This suggests that stable HRs of black carrots have been developed.

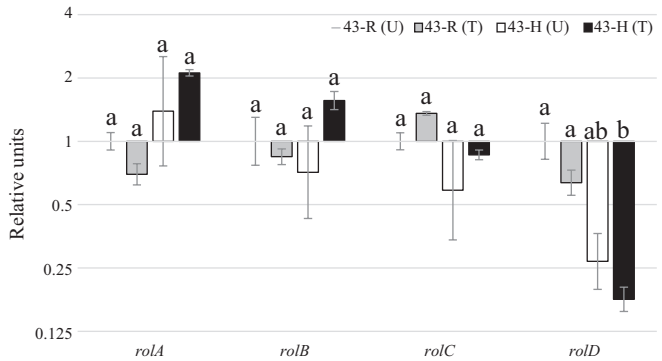

Fig. 12. Effects of ethephon treatment on the relative expression of *rol* genes in the hairy roots of lines 43-H and 43-R at day 15. Results are expressed relative to untreated 43-R [43-R (U)] as a normalizing sample. U, untreated hairy roots; T, 200 mg l^{-1} ethephon-treated hairy roots. Data represent the mean ±SE, n=3. Different letters on the top of columns indicate significant differences between the treatments and hairy root lines for each *rol* gene according to Tukey's test ($P \leq 0.05$).

However, Guivarc'h *et al.* (1999) reported an unstable phenotype and genotype of HRs of *D. carota* during a 2 year follow-up. On the other hand, other authors reported metabolic and genetic stability of *C. roseus* (Peebles *et al.*, 2009) and *Datura stramonium* HRs (Maldonado-Mendoza *et al.*, 1993) during 5 years. The longest follow-up of a HR line was in HRs of *Hyoscyamus muticus* which were subcultured during 16 years with minor fluctuations of metabolite yield (Häkkinen *et al.*, 2016).

Conclusion

This study has established, for the first time, anthocyanin-accumulating HR cultures from black carrot. The superior HR lines displayed a 25- to 30-fold biomass increase during the course of 28 d, a rate comparable with the highest reported in flasks. Ethephon acted as an efficient elicitor of anthocyanin accumulation in the selected lines, reaching an increase of up to 82% upon elicitation. An interplay between SOD activity and anthocyanin in the maintenance of redox homeostasis is suggested. Moreover, a correlation between anthocyanin content and GST could link to the function of the latter as an anthocyanin transporter. Beyond the practical implications of black carrot HRs as a bio-based system for anthocyanin production, this work provides a valuable tool for the study of interactions between secondary and antioxidant metabolism in HR growth.

Supplementary data

The following supplementary data are available at *JXB* online.

Table S1. Annotation, accession numbers, and nucleotide sequences of primers to genes used for PCR.

Table S2. Annotation, accession number, and settings of gene-specific primers used for quantitative real-time PCR (RT-qPCR) analyses.

Table S3. Identification of hydroxycinnamic acid derivatives in the hairy root extracts of lines 43-H, 43-R, and NB-R by LC-ESI/HRMS in positive ionization mode.

Table S4. Quantification of the hydroxycinnamic acid derivatives (μg g^{-1} DW) as chlorogenic acid equivalents in the hairy root extracts of lines 43-H, 43-R, and NB-R by UPLC-PDA.

Data availability

The data supporting the findings of this study are available from the corresponding author, Gregorio Barba-Espín, upon request.

Acknowledgements

This research was funded by the Danish Ministry of Science, Innovation, and Education grant number 6111-00240B and the 'Fundación Séneca' of the Agency of Science and Technology of the Region of Murcia grant number 20405/SF/17. *Rhizobium rhizogenes* strain A4 was kindly provided by Dr David Tepfer, Laboratoire de Biologie de la Rhizosphère, INRA, Versailles, Cédex, France. Majken Madvig Jansen and Sophia Schiermacher Stavnstrup are acknowledged for their technical assistance.

Author contribution

Conceptualization, GBE, RM, HL, and JC; methodology, GBE, HL, JH, SA, JC, and RM; formal analysis, GBE, JS, and SA; investigation, GBE and SC; data curation, GBE and JS; writing—original draft preparation, GBE and SC; writing—review and editing, HL, RM, JC, JH, GBE, and SA.

References

Abbasi BH, Tian CL, Murch SJ, Saxena PK, Liu CZ. 2007. Light-enhanced caffeic acid derivatives biosynthesis in hairy root cultures of *Echinacea purpurea*. Plant Cell Reports **26**, 1367–1372.

Abdelrazek S, Simon P, Colley M, Mengiste T, Hoagland L. 2020. Crop management system and carrot genotype affect endophyte composition and *Alternaria dauci* suppression. PLoS One **15**, e0233783.

Able AJ, Sutherland MW, Guest DI. 2003. Production of reactive oxygen species during non-specific elicitation, non-host resistance and field resistance expression in cultured tobacco cells. Functional Plant Biology **30**, 91–99.

Acosta-Motos JR, Hernández JA, Álvarez S, Barba-Espín G, Sánchez-Blanco MJ. 2017. The long-term resistance mechanisms, critical irrigation threshold and relief capacity shown by *Eugenia myrtifolia* plants in response to saline reclaimed water. Plant Physiology and Biochemistry **111**, 244–256.

Ahlawat S, Saxena P, Alam P, Wajid S, Abdin MZ. 2014. Modulation of artemisinin biosynthesis by elicitors, inhibitor, and precursor in hairy root cultures of *Artemisia annua* L. Journal of Plant Interactions **9**, 821–824.

Alasalvar C, Grigor JM, Zhang D, Quantick PC, Shahidi F. 2001. Comparison of volatiles, phenolics, sugars, antioxidant vitamins, and sensory quality of different colored carrot varieties. Journal of Agricultural and Food Chemistry **49**, 1410–1416.

Algarra M, Fernandes A, Mateus N, de Freitas V, Esteves da Silva JCG, Casado J. 2014. Anthocyanin profile and antioxidant capacity of black carrots (*Daucus carota* L. ssp. *sativus* var. *atrorubens* Alef.) from Cuevas Bajas, Spain. Journal of Food Composition and Analysis **33**, 71–76.

Ali MB, Yu KW, Hahn EJ, Paek KY. 2006. Methyl jasmonate and salicylic acid elicitation induces ginsenosides accumulation, enzymatic and non-enzymatic antioxidant in suspension culture *Panax ginseng* roots in bioreactors. Plant Cell Reports **25**, 613–620.

Alpizar E, Dechamp E, Lapeyre-Montes F, Guilhaumon C, Bertrand B, Jourdan C, Lashermes P, Etienne H. 2008. *Agrobacterium rhizogenes*-transformed roots of coffee (*Coffea arabica*): conditions for long-term proliferation, and morphological and molecular characterization. Annals of Botany **101**, 929–940.

Baranski R, Klocke E, Schumann G. 2006. Green fluorescent protein as an efficient selection marker for *Agrobacterium rhizogenes* mediated carrot transformation. Plant Cell Reports **25**, 190–197.

Barba-Espín G, Glied S, Crocoll C, Dzhanfezova T, Joernsgaard B, Okkels F, Lütken H, Müller R. 2017. Foliar-applied ethephon enhances the content of anthocyanin of black carrot roots (*Daucus carota* ssp. *sativus* var. *atrorubens* Alef.). BMC Plant Biology **17**, 70.

Barba-Espin G, Glied-Olsen S, Dzhanfezova T, Joernsgaard B, Lütken H, Müller R. 2018. Preharvest application of ethephon and postharvest UV-B radiation improve quality traits of beetroot (*Beta vulgaris* L. ssp. *vulgaris*) as source of colourant. BMC Plant Biology **18**, 316.

Barba-Espin G, Nicolas E, Almansa MS, Cantero-Navarro E, Albacete A, Hernández JA, Díaz-Vivancos P. 2012. Role of thioproline on seed germination: interaction ROS–ABA and effects on antioxidative metabolism. Plant Physiology and Biochemistry **59**, 30–36.

Bartling D, Radzio R, Steiner U, Weiler EW. 1993. A glutathione S-transferase with glutathione-peroxidase activity from *Arabidopsis thaliana*. Molecular cloning and functional characterization. European Journal of Biochemistry **216**, 579–586.

Behrens CE, Smith KE, Iancu CV, Choe JY, Dean JV. 2019. Transport of anthocyanins and other flavonoids by the Arabidopsis ATP-binding cassette transporter AtABCC2. Scientific Reports **9**, 437.

Bourgaud F, Gravot A, Milesi S, Gontier E. 2001. Production of plant secondary metabolites: a historical perspective. Plant Science **161**, 839–851.

Bradford MM. 1976. A rapid and sensitive method for the quantitation of microgram quantities of protein utilizing the principle of protein–dye binding. Analytical Biochemistry **72**, 248–254.

Bulgakov VP, Aminin DL, Shkryl YN, Gorpenchenko TY, Veremeichik GN, Dmitrenok PS, Zhuravlev YN. 2008. Suppression of reactive oxygen species and enhanced stress tolerance in *Rubia cordifolia* cells expressing the *rolC* oncogene. Molecular Plant-Microbe Interactions **21**, 1561–1570.

Capone I, Spanò L, Cardarelli M, Bellincampi D, Petit A, Costantino P. 1989. Induction and growth properties of carrot roots with different complements of *Agrobacterium rhizogenes* T-DNA. Plant Molecular Biology **13**, 43–52.

Cardarelli M, Mariotti D, Pomponi M, Spanò L, Capone I, Costantino P. 1987. *Agrobacterium rhizogenes* T-DNA genes capable of inducing hairy root phenotype. Molecular & General Genetics **209**, 475–480.

Carocho M, Barreiro MF, Morales P, Ferreira I. 2014. Adding molecules to food, pros and cons: a review on synthetic and natural food additives. Comprehensive Reviews in Food Science and Food Safety **13**, 377–399.

Carter C, Pan S, Zouhar J, Avila EL, Girke T, Raikhel NV. 2014. The vegetative vacuole proteome of *Arabidopsis thaliana* reveals predicted and unexpected proteins. The Plant Cell **16**, 3285–3303.

Ceoldo S, Toffali K, Mantovani S, Baldan G, Levi M, Guzzo F. 2009. Metabolomics of *Daucus carota* cultured cell lines under stressing conditions reveals interactions between phenolic compounds. Plant Science **176**, 553–565.

Chalker-Scott L. 1999. Environmental significance of anthocyanins in plant stress responses. Photochemistry and Photobiology **70**, 1–9.

Chambers MC, Maclean B, Burke R, *et al.* 2012. A cross-platform toolkit for mass spectrometry and proteomics. Nature Biotechnology **30**, 918–920.

Christensen BC, Houseman EA, Marsit CJ, *et al.* 2009. Aging and environmental exposures alter tissue-specific DNA methylation dependent upon CpG island context. PLoS Genetics **5**, e1000602.

Christensen B, Sriskandarajah S, Serek M, Müller R. 2008. Transformation of *Kalanchoe blossfeldiana* with *rol*-genes is useful in molecular breeding towards compact growth. Plant Cell Reports **27**, 1485–1495.

Christey MC, Braun RH. 2005. Production of hairy root cultures and transgenic plants by *Agrobacterium rhizogenes*-mediated transformation. Methods in Molecular Biology **286**, 47–60.

Clemente-Moreno MJ, Díaz-Vivancos P, Barba-Espín G, Hernández JA. 2009. Benzothiadiazole and l-2-oxothiazolidine-4-carboxylic acid reduce the severity of Sharka symptoms in pea leaves: effect on antioxidative metabolism at the subcellular level. Plant Biology **12**, 88–97.

Cortez R, Luna-Vital DA, Margulis D, Gonzalez de Mejía E. 2016. Natural pigments: stabilization methods of anthocyanins for food applications. Comprehensive Reviews in Food Science and Food Safety **16**, 180–198.

Desmet S, Dhooghe E, De Keyser E, Van Huylenbroeck J, Müller R, Geelen D, Lütken H. 2020. Rhizogenic agrobacteria as an innovative tool for plant breeding: current achievements and limitations. Applied Microbiology and Biotechnology **104**, 2435–2451.

Díaz-Vivancos P, Barba-Espín G, Clemente-Moreno MJ, Hernández JA. 2010. Characterization of the antioxidant system during the vegetative development of pea plants. Biologia Plantarum **54**, 76–82.

Dixon DP, Hawkins T, Hussey PJ, Edwards R. 2009. Enzyme activities and subcellular localization of members of the Arabidopsis glutathione transferase superfamily. Journal of Experimental Botany **60**, 1207–1218.

Edwards R, Dixon DP, Walbot V. 2000. Plant glutathione S-transferases: enzymes with multiple functions in sickness and in health. Trends in Plant Science **5**, 193–198.

Fenger JA, Moloney M, Robbins RJ, Collins TM, Dangles O. 2019. The influence of acylation, metal binding and natural antioxidants on the thermal stability of red cabbage anthocyanins in neutral solution. Food & Function **10**, 6740–6751.

Foyer CH, Noctor G. 2011. Ascorbate and glutathione: the heart of the redox hub. Plant Physiology **155**, 2–18.

Furner I, Huffman G, Amasino R, Garfinkel DJ, Gordon MP, Nester EW. 1986. An *Agrobacterium* transformation in the evolution of the genus *Nicotiana*. Nature **319**, 422–427.

Gautam S, Mishra A, Tiwari A. 2011. *Catharanthus* alkaloids and their enhanced production using elicitors: a review. International Journal of Pharmacy and Technology **3**, 713–724.

Georgiev MI, Agostini E, Ludwig-Müller J, Xu J. 2012. Genetically transformed roots: from plant disease to biotechnological resource. Trends in Biotechnology **30**, 528–537.

Giri A, Narasu ML. 2000. Transgenic hairy roots. Recent trends and applications. Biotechnology Advances **18**, 1–22.

Giri A, Ravindra ST, Dhingra V, Narasu ML. 2001. Influence of different strains of *Agrobacterium rhizogenes* on induction of hairy roots and artemisinin production in *Artemisia annua*. Current Science **81**, 378–382.

Giusti MM, Wrolstad RE. 2003. Acylated anthocyanins from edible sources and their applications in food systems. Biochemical Engineering Journal **14**, 217–225.

Goel MK, Mehrotra S, Kukreja AK. 2011. Elicitor-induced cellular and molecular events are responsible for productivity enhancement in hairy root cultures: an insight study. Applied Biochemistry and Biotechnology **165**, 1342–1355.

Goupy P, Dufour C, Loonis M, Dangles O. 2003. Quantitative kinetic analysis of hydrogen transfer reactions from dietary polyphenols to the DPPH radical. Journal of Agricultural and Food Chemistry **51**, 615–622.

Guerriero G, Berni R, Muñoz-Sanchez JA, *et al.* 2018. Production of plant secondary metabolites: examples, tips and suggestions for biotechnologists. Genes (Basel) **9**, E309.

Guivarc'h A, Boccara M, Prouteau M, Chriqui D. 1999. Instability of phenotype and gene expression in long-term culture of carrot hairy root clones. Plant Cell Reports **19**, 43–50.

Gutierrez-Valdes N, Häkkinen ST, Lemasson C, Guillet M, Oksman-Caldentey KM, Ritala A, Cardon F. 2020. Hairy root cultures—a versatile tool with multiple applications. Frontiers in Plant Science **11**, 33.

Häkkinen ST, Moyano E, Cusidó RM, Oksman-Caldentey KM. 2016. Exploring the metabolic stability of engineered hairy roots after 16 years maintenance. Frontiers in Plant Science **7**, 1486.

Häkkinen ST, Oksman-Caldentey KM. 2018. Progress and prospects of hairy root research. In: Srivastava V, Mehrotra S, Mishra S, eds. Hairy roots: an effective tool of plant biotechnology. Singapore: Springer, 3–19.

Hegelund JN, Lauridsen UB, Wallström SV, Müller R, Lütken H. 2017. Transformation of *Campanula* by wild type *Agrobacterium rhizogenes*. Euphytica **213**, 51.

Heazlewood JL, Tonti-Filippini JS, Gout AM, Day DA, Whelan J, Millar AH. 2004. Experimental analysis of the Arabidopsis mitochondrial proteome highlights signaling and regulatory components, provides assessment of targeting prediction programs, and indicates plant-specific mitochondrial proteins. The Plant Cell **16**, 241–256.

Huda-Faujan N, Noriham A, Abdullah Sani N, Babji AS. 2009. Antioxidant activity of plants methanolic extracts containing phenolic compounds. African Journal of Biotechnology **8**, 484–489.

Huerta-Heredia AA, Marín-López R, Ponce-Noyola T, Cerda-García-Rojas CM, Trejo-Tapia G, Ramos-Valdivia AC. 2009. Oxidative stress induces alkaloid production in *Uncaria tomentosa* root and cell cultures in bioreactors. Engineering in Life Sciences **9**, 211–218.

Jouanin L, Guerche P, Pamboukdjian N, Tourneur C, Casse Delbart F, Tourneur J. 1987. Structure of T-DNA in plants regenerated from roots transformed by *Agrobacterium rhizogenes* strain A4. Molecular and General Genetics **206**, 387–392.

Kammerer D, Carle R, Schieber A. 2003. Detection of peonidin and pelargonidin glycosides in black carrots (*Daucus carota* ssp. *sativus* var. *atrorubens* Alef.) by high-performance liquid chromatography/electrospray ionization mass spectrometry. Rapid Communications in Mass Spectrometry **17**, 2407–2412.

Kammerer DR, Carle R, Schieber A. 2004. Characterization of phenolic acids in black carrots (*Daucus carota* ssp *sativus* var. *atrorubens* Alef.) by high-performance liquid chromatography/electrospray ionization mass spectrometry. Rapid Communications in Mass Spectrometry **18**, 1331–1340.

Kessner D, Chambers M, Burke R, Agus D, Mallick P. 2008. ProteoWizard: open source software for rapid proteomics tools development. Bioinformatics **24**, 2534–2536.

Kombrink E, Hahlbrock K. 1986. Responses of cultured parsley cells to elicitors from phytopathogenic fungi: timing and dose dependency of elicitor-induced reactions. Plant Physiology **81**, 216–221.

Kondo O, Honda H, Taya M, Kobayashi T. 1989. Comparison of growth properties of carrot hairy root in various bioreactors. Applied Microbiology and Biotechnology **32**, 291–294.

Kyndt T, Quispe D, Zhai H, Jarret R, Ghislain M, Liu Q, Gheysen G, Kreuze JF. 2015. The genome of cultivated sweet potato contains *Agrobacterium* T-DNAs with expressed genes. Proceedings of the National Academy of Sciences, USA **112**, 5844–5849.

Li X, Thwe AA, Park CH, Kim SJ, Arasu MV, Al-Dhabi NA, Lee SL, Park SU. 2017. Ethephon-induced phenylpropanoid accumulation and related gene expression in tartary buckwheat (*Fagopyrum tataricum* (L.) Gaertn.) hairy root. Biotechnology & Biotechnological Equipment **3**, 1–8.

Liland KH, Almøy T, Mevik BH. 2010. Optimal choice of baseline correction for multivariate calibration of spectra. Applied Spectroscopy **64**, 1007–1016.

Lütken H, Clarke JL, Müller R. 2012. Genetic engineering and sustainable production of ornamentals: current status and future directions. Plant Cell Reports **31**, 1141–1157.

Maldonado-Mendoza IE, Ayora-Talavera T, Loyola-Vargas VM. 1993. Establishment of hairy root cultures of *Datura stramonium*. Characterization and stability of tropane alkaloid production during long periods of subculturing. Plant Cell, Tissue and Organ Culture **33**, 321–329.

Matveeva TV, Bogomaz DI, Pavlova OA, Nester EW, Lutova LA. 2012. Horizontal gene transfer from genus *Agrobacterium* to the plant *Linaria* in nature. Molecular Plant-Microbe Interactions **25**, 1542–1551.

Matveeva TV, Otten L. 2019. Widespread occurrence of natural genetic transformation of plants by *Agrobacterium*. Plant Molecular Biology **101**, 415–437.

Mishra BN, Ranjan R. 2008. Growth of hairy-root cultures in various bioreactors for the production of secondary metabolites. Biotechnology and Applied Biochemistry **49**, 1–10.

Mittler R. 2002. Oxidative stress, antioxidants and stress tolerance. Trends in Plant Science **7**, 405–410.

Mittler R, Vanderauwera S, Gollery M, Van Breusegem F. 2004. Reactive oxygen gene network of plants. Trends in Plant Science **9**, 490–498.

Montilla EC, Arzaba MR, Hillebrand S, Winterhalter P. 2011. Anthocyanin composition of black carrot (*Daucus carota* ssp. *sativus* var. *atrorubens* Alef.) cultivars Antonina, Beta Sweet, Deep Purple, and Purple Haze. Journal of Agricultural and Food Chemistry **59**, 3385–3390.

Moriuchi H, Okamoto C, Nishihama R, Yamashita I, Machida Y, Tanaka N. 2004. Nuclear localization and interaction of RolB with plant 14-3-3 proteins correlates with induction of adventitious roots by the oncogene *rolB*. The Plant Journal **38**, 260–275.

Mubarakshina MM, Ivanov BN, Naydov IA, Hillier W, Badger MR, Krieger-Liszkay A. 2010. Production and diffusion of chloroplastic H_2O_2 and its implication to signalling. Journal of Experimental Botany **61**, 3577–3587.

Murashige T, Skoog F. 1962. A revised medium for rapid growth and bio assays with tobacco tissue cultures. Physiologia Plantarum **15**, 473–497.

Namdeo AG. 2004. Investigation on pilot scale bioreactor with reference to the synthesis of bioactive compounds from cell suspension cultures of *Catharanthus roseus* Linn. PhD thesis, Devi Ahilya Vishwavidyalaya University, Indore.

Nan L, Wang K, Pang B, Zhong Y, Zhang X, Li Y, Tao F, Yang R, Liu Y. 2019. Isolation and identification of endophytes from carrots. AIP Conference Proceedings **2079**, 020018.

Park SU, Lee SY. 2009. Anthraquinone production by hairy root culture of *Rubia akane* Nakai: influence of media and auxin treatment. Scientific Research and Essays **4**, 690–693.

Peebles CA, Sander GW, Li M, Shanks JV, San KY. 2009. Five year maintenance of the inducible expression of anthranilate synthase in *Catharanthus roseus* hairy roots. Biotechnology and Bioengineering **102**, 1521–1525.

Reis L, Forney CF, Jordan M, Munro Pennell K, Fillmore S, Schemberger MO, Ayub RA. 2020. Metabolic profile of strawberry fruit ripened on the plant following treatment with an ethylene elicitor or inhibitor. Frontiers in Plant Science **11**, 995.

Sáenz-Carbonell LA, Maldonado-Mendoza IE, Moreno-Valenzula O, Ciau-Uitz R, López-Meyer M, Oropeza C, Loyola-Vargas VM. 1997. Effect of the medium pH on the release of secondary metabolites from roots

of *Datura stramonium*, *Catharanthus roseus*, and *Targetes patula* cultured *in vitro*. Applied Biochemiatry and Biotechnology **38**, 257–267.

Savitha BC, Thimmaraju R, Bhagyalakshmi N, Ravishankar GA. 2006. Different biotic and abiotic elicitors influence betalain production in hairy root cultures of *Beta vulgaris* in shake-flask and bioreactor. Process Biochemistry **41**, 50–60.

Sevón N, Oksman-Caldentey KM. 2002. *Agrobacterium rhizogenes*-mediated transformation: root cultures as a source of alkaloids. Planta Medica **68**, 859–868.

Shkryl YN, Veremeichik GN, Bulgakov VP, Tchernoded GK, Mischenko NP, Fedoreyev SA, Zhuravlev YN. 2007. Individual and combined effects of the *rolA*, *B*, and *C* genes on anthraquinone production in *Rubia cordifolia* transformed calli. Biotechnology and Bioengineering **100**, 118–125.

Sircar D, Roychowdhury A, Mitra A. 2007. Accumulation of p-hydroxybenzoic acid in hairy roots of *Daucus carota*. Journal of Plant Physiology **164**, 1358–1366.

Sivanandhan G, Dev GK, Jeyaraj M, Rajesh M, Arjunan A, Muthuselvam M, Manickavasagam M, Selvaraj N, Ganapathi A. 2013. Increased production of withanolide A, withanone, and withaferin A in hairy root cultures of *Withania somnifera* (L.) Dunal elicited with methyl jasmonate and salicylic acid. Plant Cell, Tissue and Organ Culture **114**, 121–129.

Slightom JL, Durand-Tardif M, Jouanin L, Tepfer D. 1986. Nucleotide sequence analysis of TL-DNA of *Agrobacterium rhizogenes* agropine type plasmid. Identification of open reading frames. Journal of Biological Chemistry **261**, 108–121.

Smith CA, Want EJ, O'Maille G, Abagyan R, Siuzdak G. 2006. XCMS: processing mass spectrometry data for metabolite profiling using nonlinear peak alignment, matching, and identification. Analytical Chemistry **78**, 779–787.

Srivastava S, Srivastava AK. 2007. Hairy root culture for mass-production of high-value secondary metabolites. Critical Reviews in Biotechnology **27**, 29–43.

Sroka Z, Cisowski W. 2003. Hydrogen peroxide scavenging, antioxidant and anti-radical activity of some phenolic acids. Food and Chemical Toxicology **41**, 753–758.

Stintzing FC, Carle R. 2004. Functional properties of anthocyanins and betalains in plants, food, and in human nutrition. Trends in Food Science & Technology **15**, 19–38.

Surette MA, Sturz AV, Lada R, Nowak J. 2003. Bacterial endophytes in processing carrots (*Daucus carota* L. var. *sativus*): their localization, population density, biodiversity and their effects on plant growth. Plant and Soil **25**, 381–390.

Tanaka Y, Sasaki N, Ohmiya A. 2008. Biosynthesis of plant pigments: anthocyanins, betalains and carotenoids. The Plant Journal **54**, 733–749.

Tautenhahn R, Böttcher C, Neumann S. 2008. Highly sensitive feature detection for high resolution LC/MS. BMC Bioinformatics **9**, 504.

Tepfer D. 1984. Transformation of several species of higher plants by *Agrobacterium rhizogenes*: sexual transmission of the transformed genotype and phenotype. Cell **37**, 959–967.

Toguri T, Umemoto N, Kobayashi O, Ohtani T. 1993. Activation of anthocyanin synthesis genes by white light in eggplant hypocotyl tissues, and identification of an inducible P-450 cDNA. Plant Molecular Biology **23**, 933–946.

Vasconsuelo AA, Giuletti AM, Picotto G, Rodríguez-Talou J, Boland R. 2003. Involvement of the PLC/PKC pathway in chitosan-induced anthraquinone production by *Rubia tinctorum* L. cell cultures. Plant Science **165**, 429–436.

Wang GL, Tian C, Jiang Q, Xu ZS, Wang F, Xiong AS. 2016. Comparison of nine reference genes for real-time quantitative PCR in roots and leaves during five developmental stages in carrot (*Daucus carota* L.). Journal of Horticultural Science and Biotechnology **91**, 264–270.

White FF, Taylor BH, Huffman GA, Gordon MP, Nester EW. 1985. Molecular and genetic analysis of the transferred DNA regions of the root-inducing plasmid of *Agrobacterium rhizogenes*. Journal of Bacteriology **164**, 33–44.

Yamasaki H, Sakihama Y, Ikehara N. 1997. Flavonoid-peroxidase reaction as a detoxification mechanism of plant cells against H_2O_2. Plant Physiology **115**, 1405–1412.

Yan Q, Shi M, Ng J, Wu JY. 2006. Elicitor-induced rosmarinic acid accumulation and secondary metabolism enzyme activities in *Salvia miltiorrhiza* hairy root. Plant Sciences **170**, 853–858.

Yin S, Liang Y, Gao W, Wang J, Jing S, Zhang Y, Liu H. 2013. Influence of medium salt strength and nitrogen source on biomass and metabolite accumulation in adventitious root cultures of *Pseudostellaria heterophylla*. Acta Physiologiae Plantarum **35**, 2623–2628.

Yu KW, Hahn EJ, Paek KY. 2000. Production of adventitious ginseng roots using bioreactors. Korean Journal of Plant Tissue Culture **27**, 309–315.

Yu KW, Murthy HN, Hahna EJ, Paeka KY. 2005. Ginsenoside production by hairy root cultures of *Panax ginseng*: influence of temperature and light quality. Biochemical Engineering Journal **23**, 53–56.

Zhao D, Fu C, Chen Y, Ma F. 2004. Transformation of *Saussurea medusa* for hairy roots and jaceosidin production. Plant Cell Reports **23**, 468–474.

Zhao J. 2015. Flavonoid transport mechanisms: how to go, and with whom. Trends in Plant Science **20**, 576–585.

Zybailov B, Rutschow H, Friso G, Rudella A, Emanuelsson O, Sun Q, van Wijk KJ. 2008. Sorting signals, N-terminal modifications and abundance of the chloroplast proteome. PLoS One **3**, e1994.